



Norwegian University of
Science and Technology

Prediction of Surge and Swab from Field Data Compared with Existing Theory

Analysis of Two Wells in the North Sea

Alhild Tveit

Petroleum Geoscience and Engineering

Submission date: June 2016

Supervisor: Sigve Hovda, IPT

Norwegian University of Science and Technology
Department of Petroleum Engineering and Applied Geophysics

Preface

This master's thesis is the final work of a Master of Science degree in Petroleum Technology, at the Department of Petroleum Engineering and Applied Geophysics at the Norwegian University of Science and Technology (NTNU) in Trondheim, Norway.

First I would like to thank my supervisor, associate professor Sigve Hovda for his guidance and support throughout the work with this thesis. His follow-up and theoretical knowledge has been essential to the outcome of my work. I also want to thank associate professor Pål Skalle for providing data needed for this master thesis.

A warm and special thanks to all my fellow students for all interesting discussions and feedbacks. I also want to thank my parents which has been encouraging and supportive throughout the five years at NTNU.

Alfhild Tveit

Trondheim, June 2016

Abstract

The purpose of this master thesis is to examine whether or not existing methods can be used for calculations of surge and swab pressure. Field data from two wells in the North Sea are analyzed through logs. A correlation between rapid change in block position and a corresponding alteration in standpipe pressure indicate intervals of surge and swab as long as the other relevant parameters are kept constant. Field data is taken from these intervals and the pressure is calculated using existing theory of surge and swab.

Events of surge and swab were only observed in one section. The intervals where surge and swab are observed are described by operations in the well. Different formations cause different problems and reasons for surge and swab to occur. Calculations of the pressure indicate that simplifying assumptions and other contribution effects might explain why the calculated pressure deviate from the field data.

Sammendrag

Hensikten med denne masteroppgaven er å undersøke hvorvidt eksisterende metoder kan anvendes til å beregne surge og swab. Sanntidsdata fra to brønner i Nordsjøen er analysert gjennom logger. En korrelasjon mellom rask endring i blokk posisjon og en tilsvarende endring i standpipe-trykk indikerer intervaller av surge og swab så lenge andre relevante parametere holdes konstante. Sanntidsdata blir deretter hentet fra intervallene og trykket blir kalkulert fra eksisterende metoder.

Surge and swab hendelser er kun observert i en seksjon. Intervallene hvor surge og swab er observert blir beskrevet av operasjoner gjort i en brønn. Ulike formasjoner fører til forskjellige problemer og grunner til at surge og swab oppstår. Kalkuleringer av trykkendringer indikerer at forenklete antakelser, og andre effekter som påvirker trykkendringen, kan forklare hvorfor den kalkulerte trykkendringen ikke samsvarer med trykket fra sanntidsdata.

Table of contents

1	Introduction.....	1
2	Background theory	3
2.1	Hagen-Poiseuille	3
2.2	Flow regimes.....	3
Laminar flow		5
Turbulent flow		5
2.3	Rheology.....	6
Newtonian liquid		6
Non-Newtonian liquid		6
3	Surge and Swab	9
3.1	Definition.....	9
3.2	Parameters affecting Surge and Swab	10
Tripping speed		10
Fluid Properties		10
Well bore geometry.....		10
3.3	Problems related to surge and swab	11
Fluid influx		11
Lost circulation		11
Kicks and blowout.....		12
3.4	Existing theory of surge and swab	13
Yield-Power-Law model.....		13
Lumped element model		15
4	Important parameters affecting standpipe pressure	17
4.1	Standpipe pressure	17
4.2	Flow rate.....	17
4.3	Block position	17
4.4	Torque	18
4.5	Rotation of drillstring.....	18
5	Comparison of surge and swab models with field data.....	19
5.1	Analysis of field data.....	19
5.2	Description of field data.....	20
Well operation.....		20
Description of surge and swab intervals.....		21
6	Result	23
6.1	Analysis of surge and swab events	23
6.2	Field data	33
6.3	Theoretical calculations of surge and swab	34
7	Discussion.....	37
7.1	Analysis of surge and swab	37
7.2	Parameters taken from the logs	37
7.3	Calculation of field data from existing theory.....	38
7.4	Further work.....	38
8	Conclusion	39

9	Nomenclature and Acronyms.....	41
10	References	43
	Appendix.....	45
A	Well data	45
	A.1 Well K 470	45
	A.2 Well K 480	48
B	Logs used for analysis	50
	B.1 Well K 470	50
	B.2 Well K 480	53

List of figures

Figure 2.1: Laminar flow.....	5
Figure 2.2: Turbulent flow.....	6
Figure 2.3: Rheological behavior of fluids – shear stress as a function of shear strain rate.....	7
Figure 3.1: Surge and swab when tripping in and tripping out of hole.	9
Figure 3.2: Fluid Influx.....	11
Figure 3.3: Lost Circulation to the formation.....	12
Figure 6.1: Observation of surge 26.12.04 at 00:11:01.	24
Figure 6.2: Observation of surge and swab in series 26.12.04 at 03:22:03.....	25
Figure 6.3: Observation of swab and surge 26.12.04 at 03:23:12.	26
Figure 6.4: Observation of swab 02.01.05 at 16:37:39.....	27
Figure 6.5: Observation of surge and swab 03.01.05 at 20:45:44.	27
Figure 6.6: Observation of surge and swab 04.01.05 at 00:28:44.	28
Figure 6.7: Observation of pack-off 07.01.05 at 22:31:57.	29
Figure 6.8: Observation of pack-off 07.01.05 at 22:31:57.	30
Figure 6.9: Observation of increase in RPM 25.12.04 at 14:15:15.	31
Figure 6.10: Observation of decrease in WOB 04.01.06 at 19:17:00.....	32

List of Tables

Table 5.1: Intervals of surge and swab observed through analysis of field data.	21
Table 6.1: Field data from analysis of surge and swab in the 8 ½ ” section in well K 480....	33
Table 6.2: Constant input data used in calculations of surge and swab pressure.	34
Table 6.3: Calculated parameters for use in calculations of surge and swab pressure.	35
Table 6.4: Calculated surge and swab pressures (Δ PS&S) and standpipe pressure difference (Δ SSP) from field data in the given intervals of surge and swab.	36

1 Introduction

Problems related to pressure in the well is one of the major causes of non-productive time. As more deep-water wells are drilled, the pressure window becomes more narrow (Crespo et al. 2012). Tripping in and tripping out of hole can cause pressure variations in the wellbore. An increase in friction pressure loss is an additional contribution to the bottom hole pressure (BHP) and can be referred to as surge pressure. In contrary to this, a decrease in friction pressure loss and a decrease in BHP is referred to as swab pressure. Surge and swab are parameters that can cause huge damages on the borehole and should therefore be avoided.

Analysis of field data can be used to predict surge and swab pressure. Surge and swab are observed in the logs where a rapid change in block position occur at the same time as an alteration in standpipe pressure (SPP). This applies as long as the other parameters in the log are kept constant. When the parameters are constant, a standard line for SPP is defined. When SPP deviates from the standard line, the other parameters in the log have to be taken into consideration and be analyzed on whether or not it is because of surge and swab.

The goal is to compare the existing theory of surge and swab pressure with field data. This will be achieved by analyzing two wells in the North Sea. Field data from the events of surge and swab will be used in the yield-power-law model to predict surge and swab pressure. The results are further discussed by analyzing the drilling operations and the assumptions made for the existing model. Prediction of surge and swab can also be found from other models. A physical drillstring model developed as a lumped element model can be analyzed with the aim to determine if experimental data from the physical drillstring model can be used in calculations of surge and swab pressure (Hovda, 2016)

In order to analyze the logs and predict surge and swab pressure, a basic understanding of flow regimes, rheology, surge and swab models and important parameters are presented.

The comparison of the existing theory and the field data are described. The results are discussed based on the operations during drilling and the assumptions made for the existing model. Finally, the experiment performed in this master thesis describe a result of how existing theory are compared with field data.

2 Background theory

2.1 Hagen-Poiseuille

Hagen-Poiseuille equation was derived independently by Hagen in 1839 and by Poiseuille in 1838. The equation gives the pressure drop of a Newtonian and incompressible fluid. The flow is laminar and the fluid flow through a long cylindrical pipe of constant cross section. The equation is a physical law in fluid dynamics and expressed by the pressure gradient

$$\Delta P = \frac{128 \mu L Q}{\pi r^4} \quad (1)$$

μ is the viscosity, L is the length of the cylindrical pipe, r is the radius and Q is the volumetric flow rate. Since the pressure gradient ΔP is inversely related to r^4 , any change in radius will result in an exponential change in the pressure gradient (Lake-Bakaar et al. 2015).

2.2 Flow regimes

There are three different flow regimes, laminar, transient and turbulent flow. Two types of flow may occur as a fluid flow through closed channels such as a pipe or between two plates. This depends on the velocity and viscosity of the fluid. Laminar and turbulent flow are the most common. Transient flow is a flow that alternates between being laminar and turbulent. The transition between the flows depend mainly on the ratio of inertial forces to viscous forces acting on a fluid element. This ratio, which is expressed for internal flow in a circular pipe, is defined by the dimensionless Reynolds number, Re , given in equation 2. (Cimbala & Cengel, 2014). The critical Reynolds number, Re_{cr} , is different for different geometries and flow conditions. Commonly, laminar flow is defined with a Reynolds number below 2300, $Re \lesssim 2300$, turbulent flow with a Reynolds number above 4000, $Re \gtrsim 4000$, and transitional in between.

$Re \lesssim 2300$	Laminar flow
$2300 \lesssim Re \lesssim 4000$	Transitional flow
$Re \gtrsim 4000$	Turbulent flow

$$Re = \frac{\rho v_{ann} d_e}{\mu} \quad (2)$$

ρ is fluid density, v_{ann} is fluid velocity in annulus, d_e is the hydraulic diameter for an annulus and μ is viscosity.

The hydraulic diameter for an annulus is given by

$$d_e = \frac{4A_{ann}}{P_{ann}} \quad (3)$$

A_{ann} is the cross-sectional area of the annulus and P_{ann} is the wetted parameter of the annulus. The final expression for the hydraulic diameter is

$$d_e = \sqrt{d_h^2 + d_p^2 - \frac{d_h^2 - d_p^2}{\ln\left(\frac{d_h^2}{d_p^2}\right)}} \quad (4)$$

where d_h is the diameter of the borehole or casing, and d_p is the outer diameter of the drillpipe. In the theory there are many different expressions for the hydraulic diameter (Bourgoyne Jr. et al. 1986). Different models can be applied when calculating surge and swab pressure. A more widely used method in the petroleum industry for calculating the hydraulic diameter is

$$d_e = d_h - d_p \quad (5)$$

The flow regime can be hard to determine in drilling operations, since parameters such as pipe vibrations, surface roughness, string rotation, pipe eccentricity and tool joints may effect the flow. If the pipes are very smooth, and flow disturbances and pipe vibrations are avoided, it should be kept in mind that laminar flow can be maintained at much higher Reynolds numbers, up to 100,000 (Bourgoyne Jr. et al. 1986).

Laminar flow

Laminar flow, also called streamline flow, is characterized by smooth streamlines and highly ordered motion (Bourgoyne Jr. et al. 1986). This is described as a flow with low velocity that tends to flow without lateral mixing. Laminar flow over a horizontal surface may be thought of as consisting of thin layers, all parallel to each other. The pressure, velocity and other flow properties will remain constant in each point in the fluid. Laminar flow is common in small flow channels, where the fluid has high viscosity and moves slowly. Example of laminar flow is oil flow in small tubes or blood flow through capillaries (Editors of Encyclopædia Britannica, 2016).

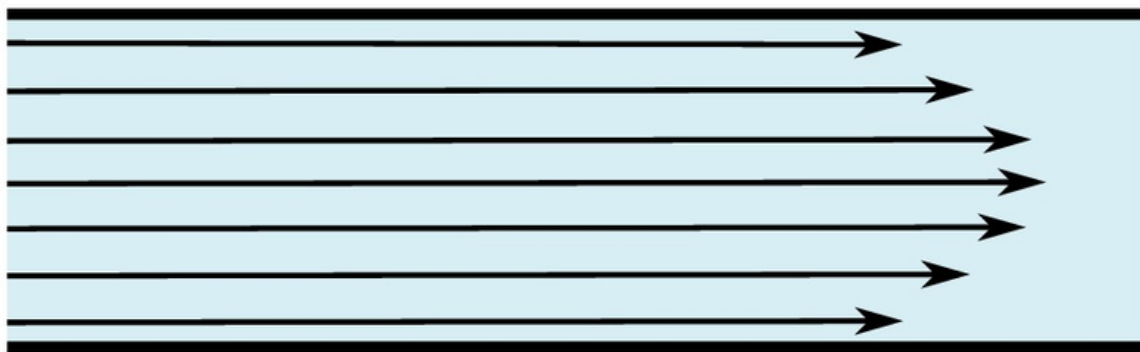


Figure 2.1: Laminar flow (CDF Support, 2016).

Turbulent flow

Turbulent flow is characterized by velocity fluctuations and highly disordered motion (Cimbala & Cengel, 2014). The velocity of the fluid at a point is continuously undergoing changes in both direction and magnitude. Most of the fluid flows are turbulent. A typically turbulent flow is low-viscosity fluid such as air at high velocities, but it can also be oil transport in pipelines and ocean currents.

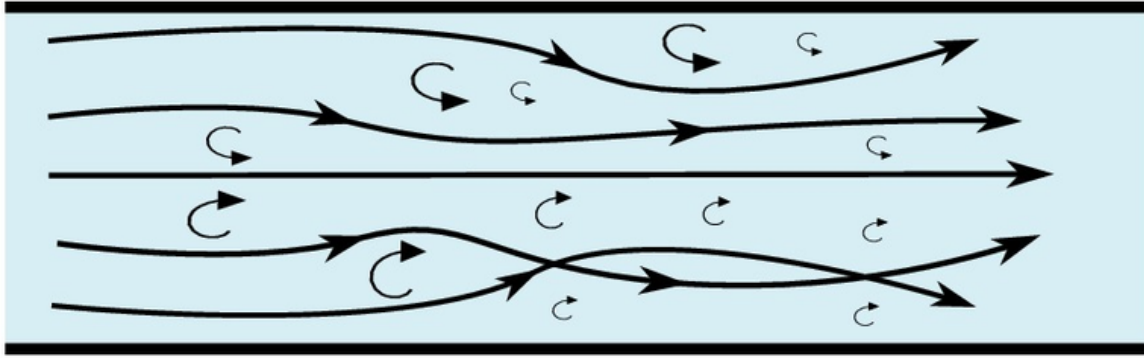


Figure 2.2: Turbulent flow (CDF Support, 2016).

2.3 Rheology

Newtonian liquid

Newtonian fluids are defined as fluids for which the shear stress is linearly proportional to the shear strain rate (Cimbala & Cengel, 2014). Air, water, honey and oil-based liquids are examples of Newtonian fluids. For these fluids, the viscosity is only dependent on temperature. The viscosity for a Newtonian fluid is constant for all shear rates and do not change with time.

Non-Newtonian liquid

When the shear stress is not linearly related to the shear strain the fluid is called a non-Newtonian fluid. The viscosity for a non-Newtonian fluid is dependent on shear rate or the deformation history. A non-Newtonian fluid will display a non-linear relation between shear stress and shear rate as seen in figure 2.3. Examples of this type of fluid is blood, paste and polymer solutions. Non-Newtonian fluids are most common and have been taken in consideration for this project. In the graph in figure 2.3 there are different types of non-Newtonian fluids.

Shear thickening fluids (dilatant fluids) becomes more viscous the more the fluid is sheared. A good example of this is quicksand. A person laying in quicksand gets more stuck the more he moves, because the viscous resistance increase.

Other fluids show the opposite effect, such as shear thinning fluids, also called pseudo plastic fluids. They become less viscous the more the fluid is sheared. Paint is a good example of a shear thinning fluid. When the paint is picked up by a brush it is very viscous as the shear rate

is small, but when the paint is applied to the wall, and the thin layer of paint between the brush and the wall is subjected to a large shear rate, it becomes less viscous.

When the shear thinning effect becomes extreme the fluids are called Bingham plastic fluids. Toothpaste is an example of Bingham plastic fluid and in some of the plastic fluids a yield stress is required before the fluid begins to flow (Cimbala & Cengel, 2014).

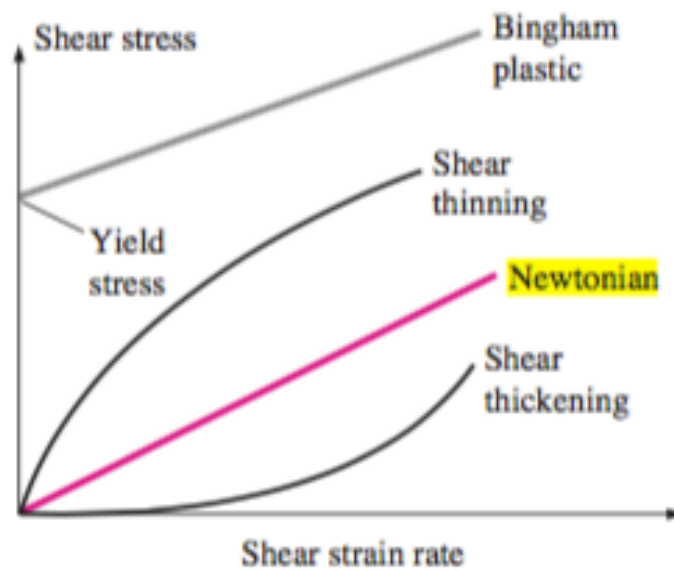


Figure 2.3: Rheological behavior of fluids – shear stress as a function of shear strain rate (Fluid Mechanics - Fundamentals and Applications, 2014).

3 Surge and Swab

3.1 Definition

The movement of the drillstring during drilling and tripping will affect the BHP. A drillstring is normally tripped out of the borehole or into the borehole during completions and workover operations. As the drillstring is run into the borehole, mud is displaced and the drillstring acts like a piston. The displaced mud causes a change in the annular velocity around the pipe, which further leads to an increase in friction pressure loss. The result of an increase in pressure at any given point in the well is referred to as surge pressure.

On the other hand, when tripping out of the hole, the drilling fluid will flow to replace the volume where the pipe has been removed. The annular flow velocity will decrease and change around the pipe, leading to decreased friction pressure loss. This is commonly called swab pressure (Skalle, 2012).

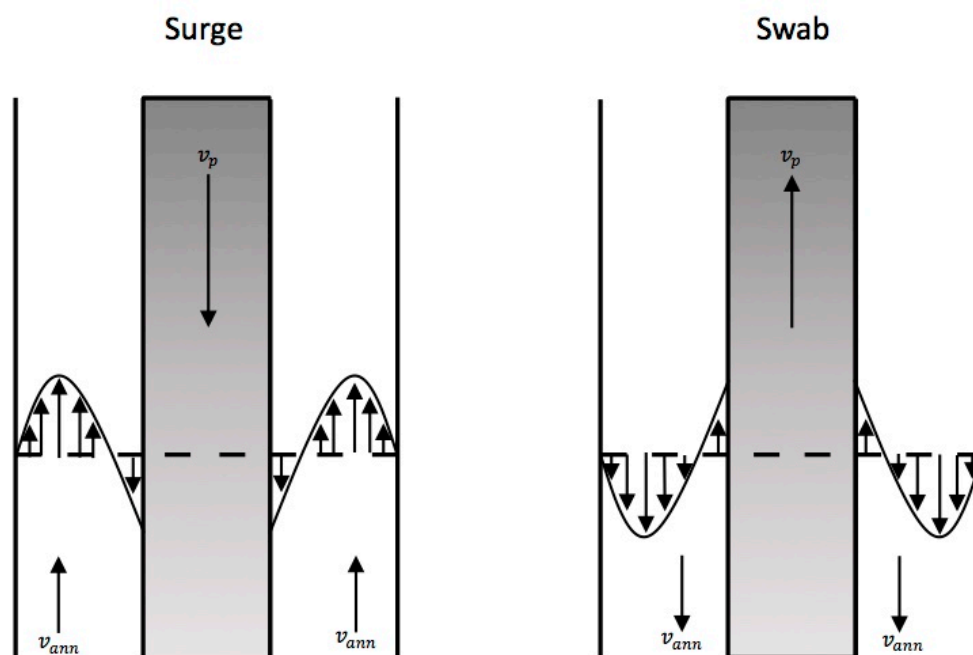


Figure 3.1: Surge and swab when tripping in and tripping out of hole.

3.2 Parameters affecting Surge and Swab

Tripping speed

The faster the pipe is moving, the greater the potential of surge and swab. High tripping speed enhances the piston effect in the well. Pål Skalle said that “Tripping speed is the only manipulative parameter with respect to controlling surge and swab pressure” (Skalle, 2012). Maximum tripping speed is important to estimate in order to keep the wellbore pressure within specific limits of the pore and fracture pressures. If the tripping speed becomes too low it can result in excessive non-productive time and increase drilling costs.

Fluid Properties

Surge and swab depends on lifting and flowing of fluid. A fluid with high viscosity makes the fluid more difficult to flow, hence a slower tripping speed is necessary to allow fluid to flow. High gel strength resist flow from static condition, and during trip-in and trip-out the likelihood of surge and swab increase. Density has the most important role in severity of surge and swab pressures (Forutan & Hashemi, 2011). A too high or a too low mud density reduces clearance and affect the tripping speed which leads to the surge and swab effect.

Well bore geometry

Clearance between the drillstring and the wellbore is critical, and the smaller the clearance, the more restriction fluid must overcome to flow. When the annular clearance decrease, the surge and swab pressure increase. Factors, such as balling, BHA length, hole angle, doglegs, salt or swelling formations and number of stabilizers affect clearance. The tripping speed is dependent on diameter ratio and annular eccentricity. Large hole size allows the drilling fluid to rapidly fill in the place that were occupied by the drillstring when tripping out of hole. The formation pore pressure can then easily be controlled and blowouts are prevented. While tripping in, a large hole will provide bigger passage area for the mud. The piston-cylinder action acting opposite to the formation is minimized and fracturing of the formation can be avoided. Eccentricity mostly affect the surge and swab pressures in inclined and horizontal wells. It is possible to move the pipe faster than predicted by concentric models and still be operating safely. This is due to the differential pressure loss is higher in a concentric annulus than in an eccentric annulus (Srivastav, 2012).

3.3 Problems related to surge and swab

Accurate prediction of surge and swab is necessary to prevent fracturing of the formation, lost circulation, excessive loss of drilling fluids, well-control problems, and increased drilling cost. Surge pressure increase BHP while swab decrease BHP.

Fluid influx

When the formation pressure gets higher than the hydrostatic pressure in the wellbore, formation fluids are allowed to enter the wellbore unintendedly. The undesirable flow is called a kick or wellbore influx. Because the hydrostatic pressure decreases when swabbing occur, it can be one of the reasons that this happens. To prevent damages, early detection of swabbing on trips is critical in order to minimize the size of an eventually kick. In worst case the kicks can result in a blowout.

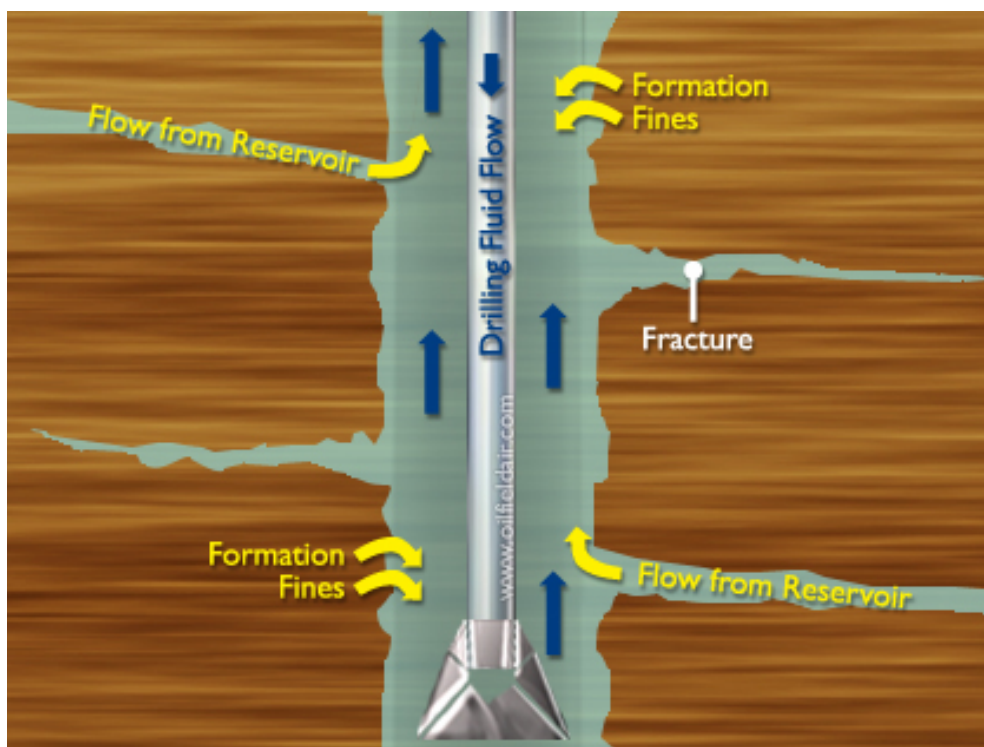


Figure 3.2: Fluid Influx (Petroleumsupport, 2011)

Lost circulation

Lost circulation is one of the main problems related to surge pressure. When the drillstring is tripped into the borehole, a pressure is created and exerted on the bottom of the well. Fluid in the well must move upward to exit the volume being entered by the drillstring. The piston effect

that occurs results in an increase in the hydrostatic pressure, also called surge pressure. When the surge pressure exceeds the formation fracture pressure it can result in fracturing of the formation and weakening. A high surge pressure can also lead to lost circulation by continuous fluid loss into the permeable formation. The mud pumped down the well will flow into the fractures and cause a reduction in the vertical height in the mud columns and a reduction in the wellbore hydrostatic pressure.

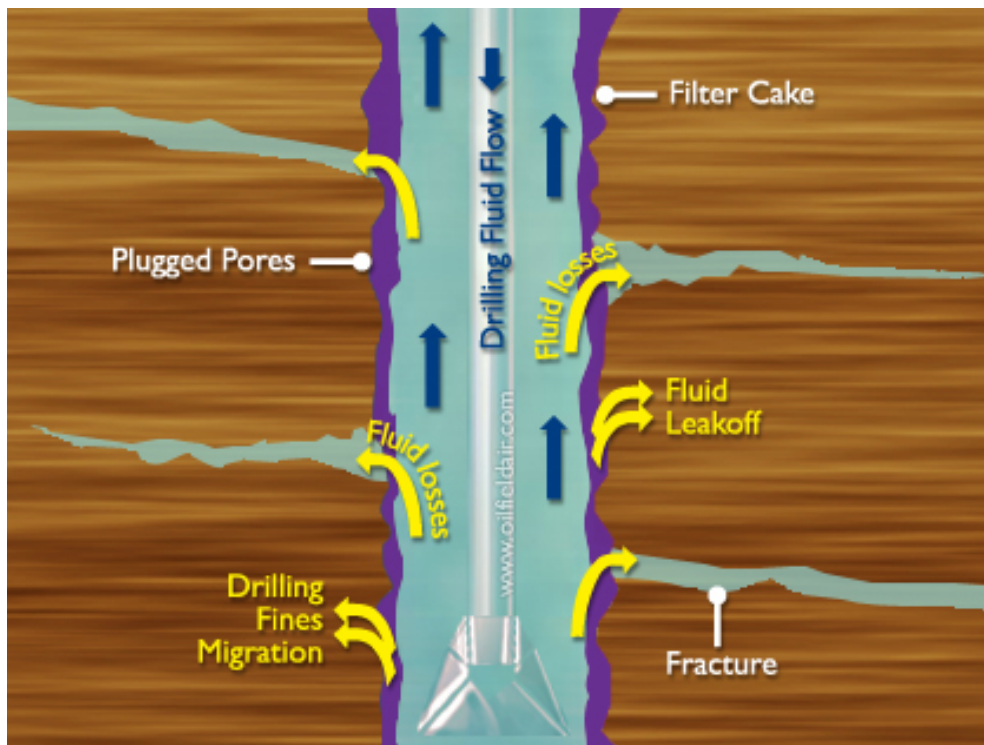


Figure 3.3: Lost Circulation to the formation (Petroleumsupport, 2011)

Kicks and blowout

A reduction of BHP can be large enough to cause an underbalanced situation in the well. As mentioned will a kick occur when formation fluid flows into the wellbore during drilling. If this flow is uncontrolled it can result in a blowout. A kick that is not controlled can lead to huge damages like loss of operation time, loss of the well, and in worst case, loss of the rig and lives of personnel.

3.4 Existing theory of surge and swab

Yield-Power-Law model

An accurate prediction of surge and swab pressure is important to keep the wellbore pressure within specified limits of the pore and fracture pressures. Different models are developed to predict downhole surge and swab pressure. The most accurate model is the yield-power-law model (YPL) that account for fluid and formation compressibility, and pipe elasticity. It also provides a better description of drilling fluids over a wide range of shear rates. Other models are based on Bingham plastic (BP) and power-law (PL) fluid rheology models that cannot sufficiently describe the flow behavior of drilling fluids.

Since surge and swab can cause such huge damages a precise prediction of surge and swab is necessary for efficient drilling operations (Crespo et al. 2012).

Surge and swab generally depends on wellbore geometry, tripping speed, fluid rheology and flow regime. Usually when calculations are done on surge and swab it is necessary to make simplifying assumptions.

In most cases the drillstring is close-ended so the added volume either occupied during surge or removed during swab can be calculated. Steady state flow conditions are considered in a concentric annular geometry. Normally, in real situations, annular geometry is not concentric and the pressure change caused by surge and swab can be reduced up to 40 % due to eccentricity (Crespo et al. 2012). All of these predictions are only valid if the tripping speed remains constant.

The YPL model for surge and swab pressure in the wellbore is given by

$$\Delta p_{s\&s} = 2f \frac{\rho(v_{ann} + \frac{v_p}{2})^2}{g(d_h - d_p)} L_p \quad (6)$$

f is the fanning friction factor, ρ is the density of the fluid, v_{ann} is the annular velocity, v_p is the tripping velocity, d_h is the diameter of the borehole or casing, d_p is the outer diameter of the drill pipe and L_p is the length of the pipe.

The fanning friction factor equation is a function of the Reynolds' number Re and the relative roughness. The relative roughness is defined as the ratio of absolute roughness ϵ , to the hydraulic diameter of an annulus (Cimbala & Cengel, 2014). Colebrook presented an empirical correlation for the determination of friction factors with a fully developed turbulent flow

$$\frac{1}{\sqrt{f}} = -4 \log \left[\frac{1.255}{Re\sqrt{f}} + 0.269 \frac{\bar{\epsilon}}{d_e} \right] \quad (7)$$

As this expression requires some iteration, S.E. Haaland developed an approximate explicit relation for f . The results obtained for f from Haaland's equation are within 2 % of those obtained from the Colebrook equation (Cimbala & Cengel, 2014).

$$\frac{1}{\sqrt{f}} = -1.8 \log \left[\frac{6.9}{Re} + \left(\frac{\bar{\epsilon}/d_e}{3.7} \right)^{1.11} \right] \quad (8)$$

$\bar{\epsilon}$ is the average absolute roughness of the pipe, d_e is the hydraulic diameter for an annulus and Re is Reynolds number which can be calculated by using equation 2.

The selection of an appropriate absolute roughness ϵ for an annulus is often difficult. The average absolute roughness of an annulus can be estimated by

$$\bar{\epsilon} = \frac{\epsilon_{oh}d_h^2 + \epsilon_p d_p^2}{d_h^2 + d_p^2} \quad (9)$$

ϵ_p is the absolute roughness of commercial steel in drillpipe and casing and ϵ_{oh} is the absolute roughness of the borehole.

In the fanning friction factor equation (8) the average absolute roughness ($\bar{\epsilon}$) divided by the hydraulic diameter (d_e) is the relative roughness (ϵ_{rel}).

$$\epsilon_{rel} = \frac{\bar{\epsilon}}{d_e} \quad (10)$$

Lumped element model

A lot of models have been developed to predict the best solution of theoretical calculation of surge and swab pressure. Existing theory discuss different assumptions for improvement of the calculations of surge and swab. The lumped element model is considered as a drillstring modelled as a set of n blocks that are connected by n springs (Hovda, 2016)

The assumptions for the model is Newtonian mud, laminar flow rate, steady, axial symmetric and all radial and swirl components are zero (Hovda, 2016). Navier-Stokes momentum equation in three dimensional cylindrical coordinates with an annulus pressure p_i that only will be a function of axial coordinate alone are reduced to

$$\frac{1}{r} \frac{\partial}{\partial r} \left(r \frac{\partial u_i}{\partial r} \right) = \frac{1}{\mu} \left(\frac{\partial p_i}{\partial z} - \rho_m g \right) \quad (11)$$

μ is viscosity, ρ_m is mud density, u_i is the axial velocity component of a fluid particle and r is the distance from the center of the hole.

By integrating this expression twice with respect to r gives

$$u_i = U_i r^2 + C_1 \ln r + C_2 \quad (12)$$

Here $U_i = \frac{(\frac{\partial p_i}{\partial z} - \rho_m g)}{(4\mu)}$ and C_1 and C_2 are constants. In order of a case with flow in a circular pipe, it is assumed that $u_i(0)$ is finite meaning $C_1 = 0$. The derivation will result in Hagen-Poiseulle law.

The annular pressure p_i can be described as

$$p_i = h \sum_{j=1}^i \frac{\partial p_j}{\partial z} = \rho_m g h_i + \frac{4\mu V h}{\pi R^4} \sum_{j=1}^i \psi_j + \frac{4\mu h}{R^2} \sum_{j=1}^i \phi_j \dot{q}_j \quad (13)$$

h is the length of each segment, g is the gravity constant, V is the flow of the mud that is pumped into the drill pipe, R is the radius of the hole, \dot{q}_j is the velocity of the drillstring at a given point and

$$\psi_j = \frac{2}{(1 - \alpha_j^4) + \frac{(1 - \alpha_j^2)^2}{\ln(\alpha_j)}}$$

$$\phi_j = \frac{-1}{(1 + \alpha_j^2) \ln(\alpha_j) + (1 - \alpha_j^2)}$$

where ψ_j and ϕ_j are always positive for $0 < \alpha_j < 1$.

In the annular pressure expression, the first term is the hydrostatic pressure, the second term is the dynamic friction term that is proportional to V . The third term is only related to the movement in the drillstring and is also a dynamic friction.

Surge and swab pressure for this model is motivated from equation 13 and is defined as

$$\Delta P_j(\tau) = \frac{4Q_s \mu h}{R^2} \exp\left(-\frac{c}{2}\tau\right) \sum_{i=1}^j \phi_j \left(\sum_{k=1}^n \frac{a_1 V_{ik} V_{1k}}{\omega_{d,k}} \sin(\omega_{d,k}\tau + C_k) \right) \quad (14)$$

Where $C_k = \cos^{-1}(\zeta_k) + \tan^{-1}\left(-\sqrt{1 - \frac{\zeta_k^2}{\omega_{d,k}^2}}\right)$.

4 Important parameters affecting standpipe pressure

While analyzing field data a lot of parameters are taken into consideration. Some parameters affect SPP pressure more than others. To evaluate SPP it is important to understand how the parameters affect the pressure and what the different parameters indicate.

4.1 Standpipe pressure

SPP is defined as the total frictional pressure drop in the hydraulic circuit. Analyzes of SPP is necessary to detect surge and swab. A standard line for SPP is defined when all of the parameters are constant. If SPP differs from this line some of the parameters are changed and downhole problems might be identified.

4.2 Flow rate

When looking for surge and swab, flow rate is one of the most important parameters to examine. Alterations in flow rate has a huge impact on SPP, as can be seen from the logs. Almost every time flow rate is changing, SPP will change immediately. Exceptions can be found in intervals where the flow rate is kept constant and there is an alteration in SPP. This can be a good indicator of surge and swab, but before any decision is taken other parameter also has to be checked.

4.3 Block position

Changes in block position is important when analyzing logs. The observation of changes in block position can tell whether or not SPP is altering because of tripping in or tripping out. However, if the change in block position is delayed, SPP might not be changed due to tripping in or tripping out nor will it be an indicator of surge and swab.

4.4 Torque

Torque is the tendency of a force to rotate an object about some axis (Serway & Jewett, 2009). When analyzing for surge and swab in the logs it is important to not confuse the observations with pack-offs. Pack-offs can be observed where a peak in the torque is observed at the same time as SPP alter from the standard line. In these events RPM is kept constant.

4.5 Rotation of drillstring

Revolutions per minute (RPM) is used to measure rotational speed. RPM can also influence SPP. Often when RPM is changed, a change in SPP is also observed. An explanation to this is the presence of helical flow patterns when RPM increase which can cause the SPP to decrease.

5 Comparison of surge and swab models with field data

5.1 Analysis of field data

Analysis of surge and swab are done on four different sections in two different wells in the North Sea. In well K 470, a 17 ½“, 12 ¼” and a 8 ½“ section are analyzed, and in K 480, a 8 ½“ section is analyzed. The sections are presented in more details in appendix A. Drawings of the well path, well data and key information are also presented.

Field data is analyzed from the logs in a matlab program developed by Verdande Technology. The logs are manually analyzed by looking at field data for the different parameters described in the previous chapter. The parameters are weight on bit (WOB), block position, SPP, flow rate, RPM and torque, where all parameters are plotted against time. In the logs they are defined as SWOB, BPOS, SPPA, TFLO, RPM and TQA, respectively. The most important parameters for indication of surge and swab are SPP, flow rate, block position and torque.

Alterations in SPP are found by defining a standard line for SPP. The standard line is defined for a constant SPP that do not diverge when any of the critical parameters are kept constant. The intervals where surge and swab are observed are manually selected based on a change in SPP. When tripping in or tripping out of the borehole, a sudden change in block position will appear. If the change in block position occurs at the same time as an alteration in SPP, it can be an indication of surge and swab. This is reasonable as long as there are no other causes of change in SPP. To investigate whether it is surge and swab or another reason for an alteration in SPP, one must to check if any of the other parameters are changed as well. Obviously, the first thing to check is the flow rate. If the flow rate is kept constant when SPP deviates from the standard line, there is an alteration in SPP. Block position is then analyzed, and as already mentioned, if there is a change in block position at the same time as an alteration in SPP it indicates surge and swab. The other parameters should still be looked into to make sure they are not affecting SPP. The logs have to be examined in seconds. By taking a closer look on both the change in block position and the change in SPP, it is found that the change in block position can be a little delayed compared to the change in SPP. When such cases arise, the torque might have changed even though RPM is kept constant. Torque, block position and flow rate are not the only factors affecting SPP. Rotation of the drillstring can also influence the SPP. When an alteration in SPP is observed just after a change in RPM, it is necessary to detect whether or not

there is a rapid change in block position. In cases where SPP is altered and non of the mentioned parameters are changing, WOB has to be checked for alterations.

5.2 Description of field data

The purpose of analyzing the field data is to find surge and swab events in the logs. These events are further discussed and analyzed by taking field data from the logs. The field data taken from the logs is used to calculate other parameters needed for estimations of surge and swab pressure. The expression given in equation 6 gives a new surge and swab pressure based on parameters found from the logs and the calculated parameters. The calculated pressure is then compared with field data. The calculations and the results of the analysis are shown in the next chapter

The results from the analysis are found in the 8 ½“ section in well K480. Some of the surge and swab events found in well K 480 are observed successively.

Well operation

Drilling data for the 8 ½“ section in well K 480 is available through information from the drilling operation. The section is drilled from 5091 mMD to 6221 mMD, so the total measured length of the interval is 1130 m. The true vertical depth of the section is from 2821 mTVD - 2895 mTVD. The well kicks off at 5120 mMD and is drilled to 5848 mMD. At this point the rotation is stopped because of noise from the derrick drilling machine (DDM) is observed. Problems with the PS AC motor occur, so a new motor has to be installed. At 5752 mMD pack-offs causes problems, but both circulation and rotation are regained. After the hole is circulated clean and a new BHA is installed, the drilling continues. In the interval between 5940 mMD and 6076 mMD, the drill bit hits hard stringers. The formation turns out to be extremely hard from 6068 mMD with a ROP of only 1-2 m/hr. From 6076 mMD to 6221 mMD the well is drilled in hard formation where the last 145 mMD is drilled with rotational steerable system (RSS). At this point there is no connection with the Xceed tool, and the angle is dropping too much. The hole is then circulated clean, and the drillstring is pulled out of the hole (POOH) to 1908 mMD. In an attempt to continue drilling, pack-off problems are experienced at 6217 mMD. It is decided to do a side track. At 5604 mMD an open hole sidetrack is performed and the sidetrack is drilled with RSS to 5878 mMD.

Description of surge and swab intervals

Investigation of drilling data is presented for each interval where surge and swab are observed. The intervals where surge and swab occur in succession are described as one interval.

Table 5.1: Intervals of surge and swab observed through analysis of field data.

Interval	Section	Event	Date [dd.mm.yy]	Time from [hh:mm:ss]	Time to [hh:mm:ss]	MD [m]
1	K 480 8 ½”	Surge	26.12.04	00:11:01	00:11:47	5823
2	K 480 8 ½”	S & S	26.12.04	03:22:03	03:25:26	5847
3	K 480 8 ½”	Swab	02.01.05	16:37:39	16:39:09	6002
4	K 480 8 ½”	S & S	03.01.05	20:45:54	20:48:54	6111
5	K 480 8 ½”	S & S	04.01.05	00:28:44	00:31:21	6128

Each section is drilled at different MD, but the total measured length is only 305 mMD between the first and the last interval. Interval 1 and 2 are observed at the same day, they are both observed during the same drilling interval. The drilling interval from 5720 mMD to 5848 mMD is drilled with 3D RSS, with a flow rate of approximately 2100 l/min and a rotation speed of 180 RPM. The lithology in interval 1 is interbedded sandstone, siltstone and claystone with stringers of limestone found from cutting samples. However, a change in lithology happens right before interval 2, so here the cutting samples only show interbedded claystone and sandstone with stringers of limestone. This type of formation is known to be very hard and the rotation stopped right after interval 2. The interval from 6002 mMD to 6069 mMD is drilled with increased WOB. This is done because a drillstring with more WOB easier drills through the hard formation. At 6002 mMD where interval 3 is located, an increase in drag occurs, and the hole is reamed for the hole stand. The lithology in interval 3 is claystone with minor amounts of limestone and sand. Interval 4 and 5 are hard to drill as the lithology indicates limestone with some clay-rich intervals and traces of sand. The occasionally hard stringers cause huge problems while drilling and at 6221 mMD it is decided to POOH.

6 Result

In this section analysis of field data from two wells in the North Sea are presented. Events of surge and swab are observed in the logs and the results are presented in graphs where alterations in SPP are clearly shown. Critical parameters, such as flow rate, block position, torque, RPM and WOB, are considered in the analysis as all of the parameters strongly affect SPP.

Alterations in SPP are found by manually searching through the logs. The observed changes in SPP are then compared with the critical parameters and analyzed to decide whether the alteration is due to surge, swab or pack-off.

Field data are taken from the sections where surge and swab are observed. The field data is then used to calculate parameters needed in the expression for surge and swab pressure. The calculations will further be compared with changes in SPP. The intervals where surge and swab are observed are presented in tables and graphs in this chapter. An overview of the logs used for the analysis can be found in appendix B.

6.1 Analysis of surge and swab events

Surge and swab are observed when there is an alteration in SPP. Alterations in SPP happen as a result of changes in one of the critical parameters. Whether it is surge, swab or pack-off depends on which parameter is causing the change in SPP, i.e. which parameter is changed at the same time as there is a change in SPP. A rapid change in block position at the same time as a change in SPP clearly indicates either surge or swab. This is due to the tripping speed exceeding the estimated maximum tripping speed (Crespo et al. 2012). Too high tripping speed can lead to variations in the wellbore pressure and the mud window might be exceeded.

Surge and swab are as already mentioned only observed in the 8 ½“ section in well K 480. Fourteen cases of surge and swab are observed in this section. The observations are divided into five intervals because in some of the intervals surge and swab are occurring in succession. Surge is observed in the first interval as shown in figure 6.1.

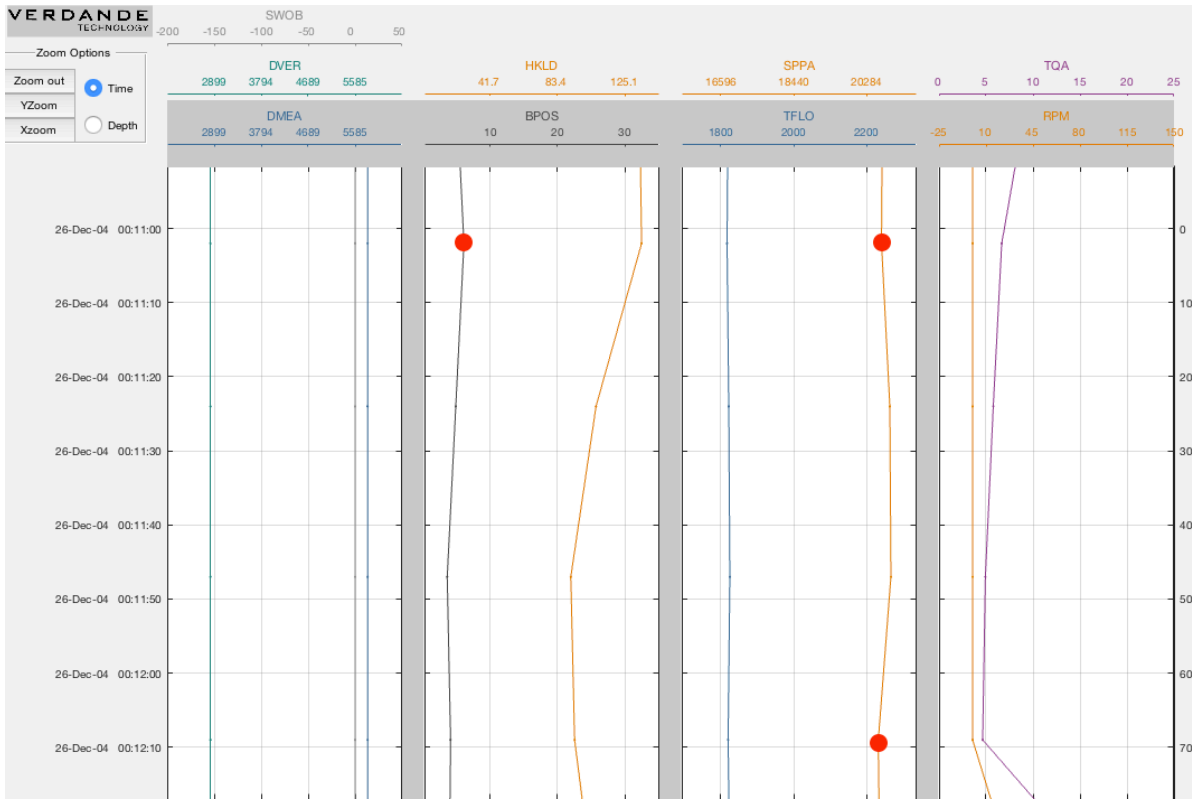


Figure 6.1: Observation of surge 26.12.04 at 00:11:01. The red circles indicate the start and end of an alteration in SPP, while the red circle on BPOS indicate where BPOS change direction.

If torque, RPM and the WOB is kept constant, it is an indication of surge. The red circles show where the alteration of SPP starts and ends. It can also be seen that a change in block position occurs at the same time as the alteration of SPP starts.

Successive intervals of surge and swab are common and can be seen where block position is changing rapidly from increasing to decreasing. This is due to wellbore geometry and cuttings accumulation when tripping out and tripping in of the hole. Figure 6.2 shows a series of surge and swab, while figure 6.3 shows a more detailed graph of one surge and one swab event and the transition between them.

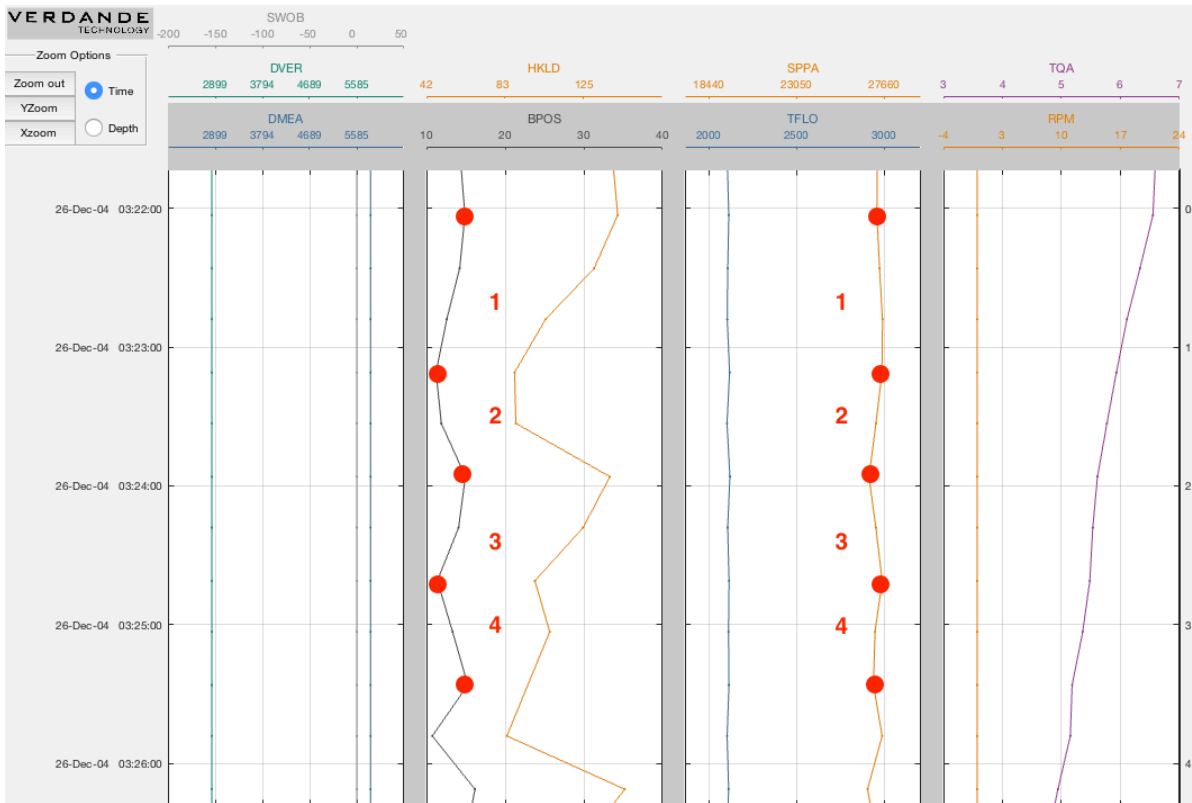


Figure 6.2: Observation of surge and swab in series 26.12.04 at 03:22:03. The first change in SPP (event 1) indicates surge as SPP increases and BPOS decreases. Event 2 is swab, event 3 is surge and event 4 is swab.

Event 1, which is a surge event, has a decreasing block position which means the drillstring is tripping into the hole. When the block position is increasing, the drillstring is tripping out of the hole. The other critical parameters are constant in this interval of surge and swab.

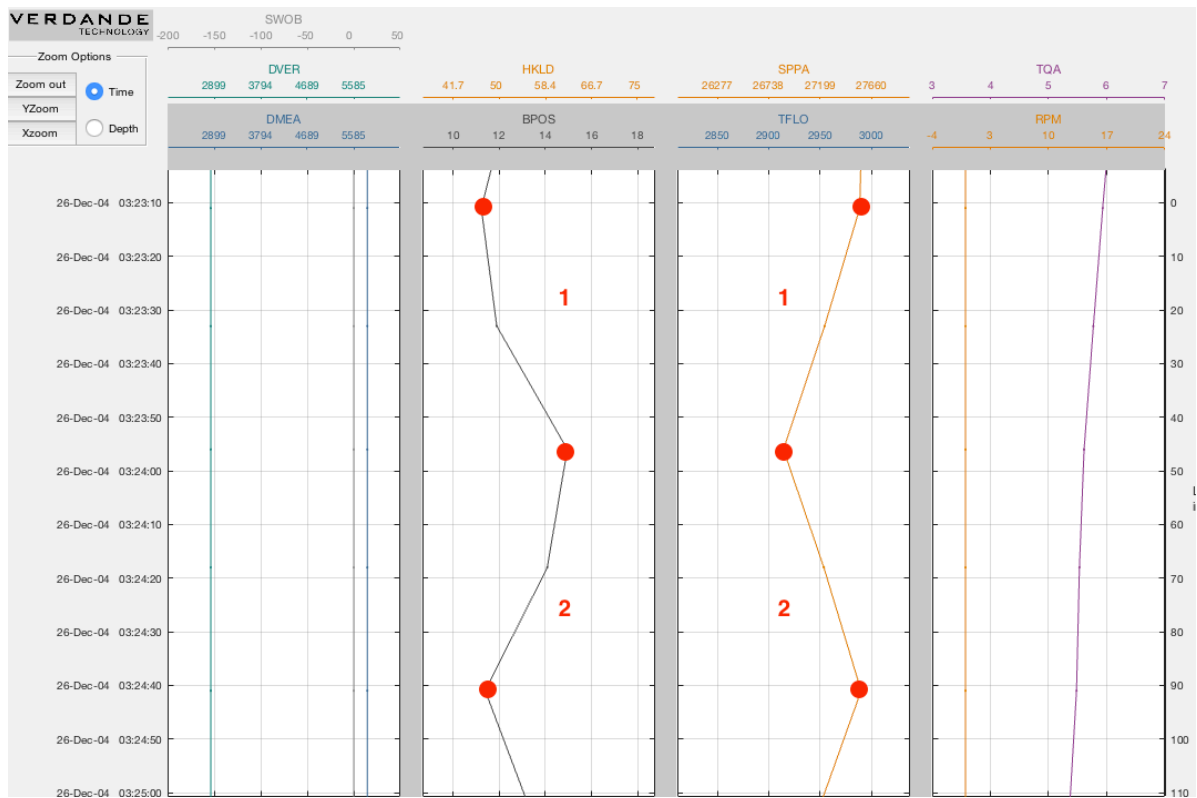


Figure 6.3: Observation of swab and surge 26.12.04 at 03:23:12. This graph does not show the flow and the hockload as figure 6.2. The graph shows a better picture of surge and swab and the transition between them. Event 1 is swab, and event 2 is surge.

There are three more intervals with surge and swab observations. Two of the intervals are surge and swab occurring in succession, and one interval is a swab observation. All of these intervals are shown in figure 6.4, figure 6.5 and figure 6.6.

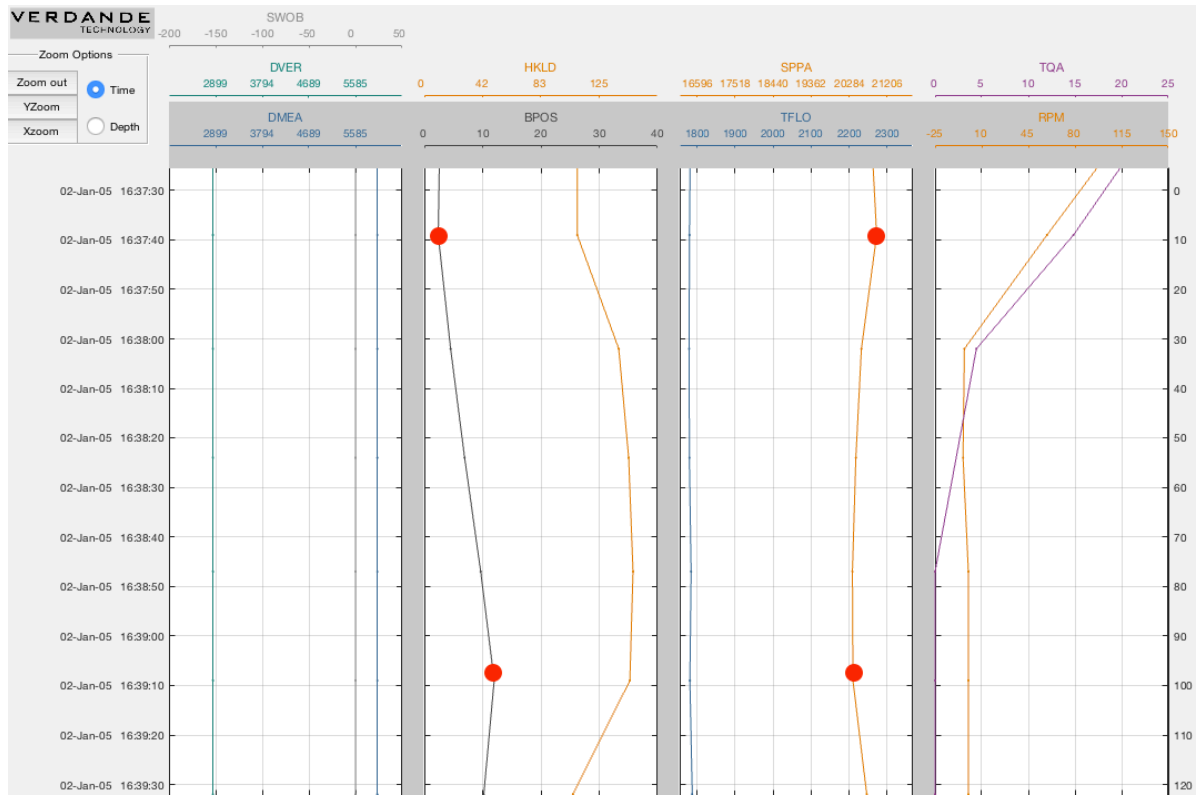


Figure 6.4: Observation of swab 02.01.05 at 16:37:39.

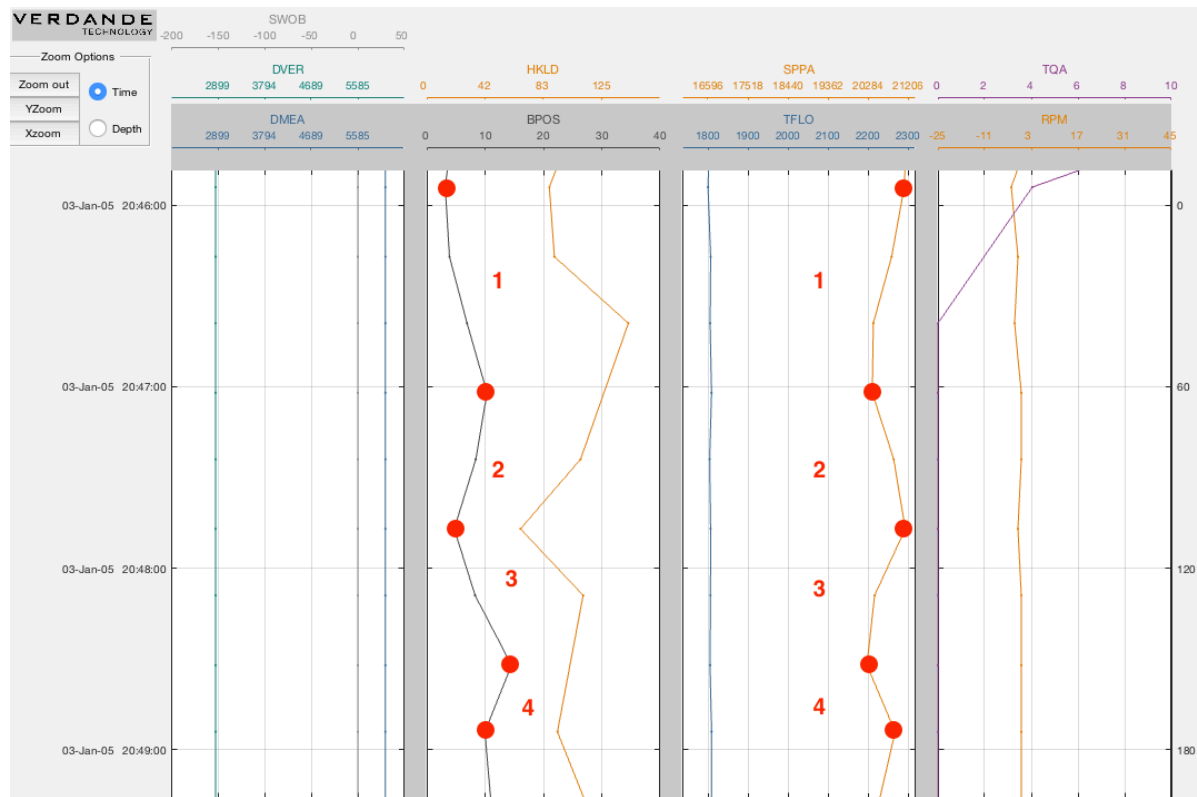


Figure 6.5: Observation of surge and swab 03.01.05 at 20:45:44.

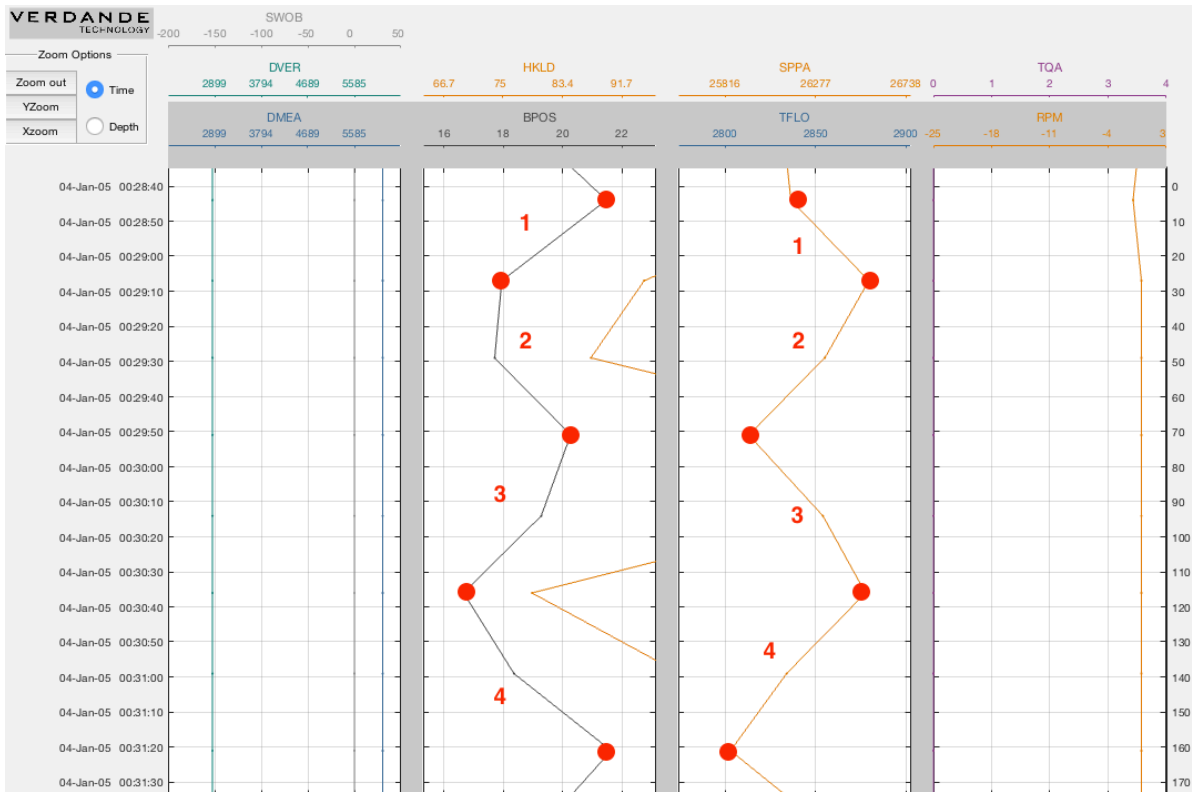


Figure 6.6: Observation of surge and swab 04.01.05 at 00:28:44. The log doesn't include TFLO, as this is constant.

From the logs it is clear that there is a pattern when surge and swab are analyzed. All of the other parameters, WOB, flow rate, torque and RPM, are kept constant and are not affecting SPP in the intervals where surge and swab are observed.

As we can see from the log showing depth and WOB, they are both constant throughout the log. This is an indication of drilling, and as already explained from the drilling data, it can be seen that every interval where surge and swab are observed are during drilling of the well.

RPM and torque are acting the same way. Since no peaks are seen in either RPM or torque, they have no impact on SPP.

A change in torque at the same time as a change in SPP is an indication of pack-off. However, this only applies when the change in block position is observed after the change in SPP.

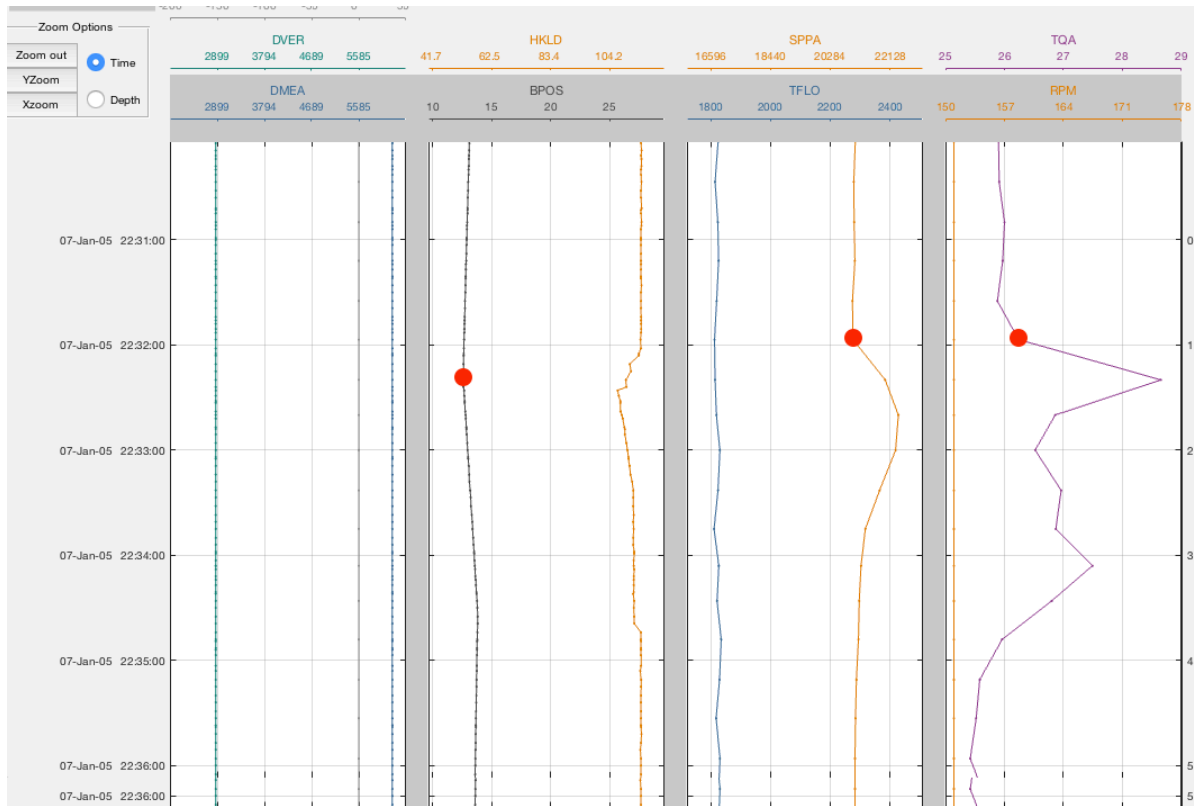


Figure 6.7: Observation of pack-off 07.01.05 at 22:31:57. The logs indicate pack-off because the alteration of TQA is observed at the same time as a change in SPP.

Pack-off can happen for a variety of reasons. The most common reasons are insufficient cuttings removal and wellbore collapse around the drillstring. The consequence is a sudden reduction in the ability of the drillstring to circulate (Schlumberger, 2016). In figure 6.7 this is shown as an alteration in SPP at the same time as an increase in torque.

The beginning of an SPP alteration is presented in more detail in figure 6.8. The torque starts to increase at the exact same time as an increase in SPP, while the block position is a little delayed.

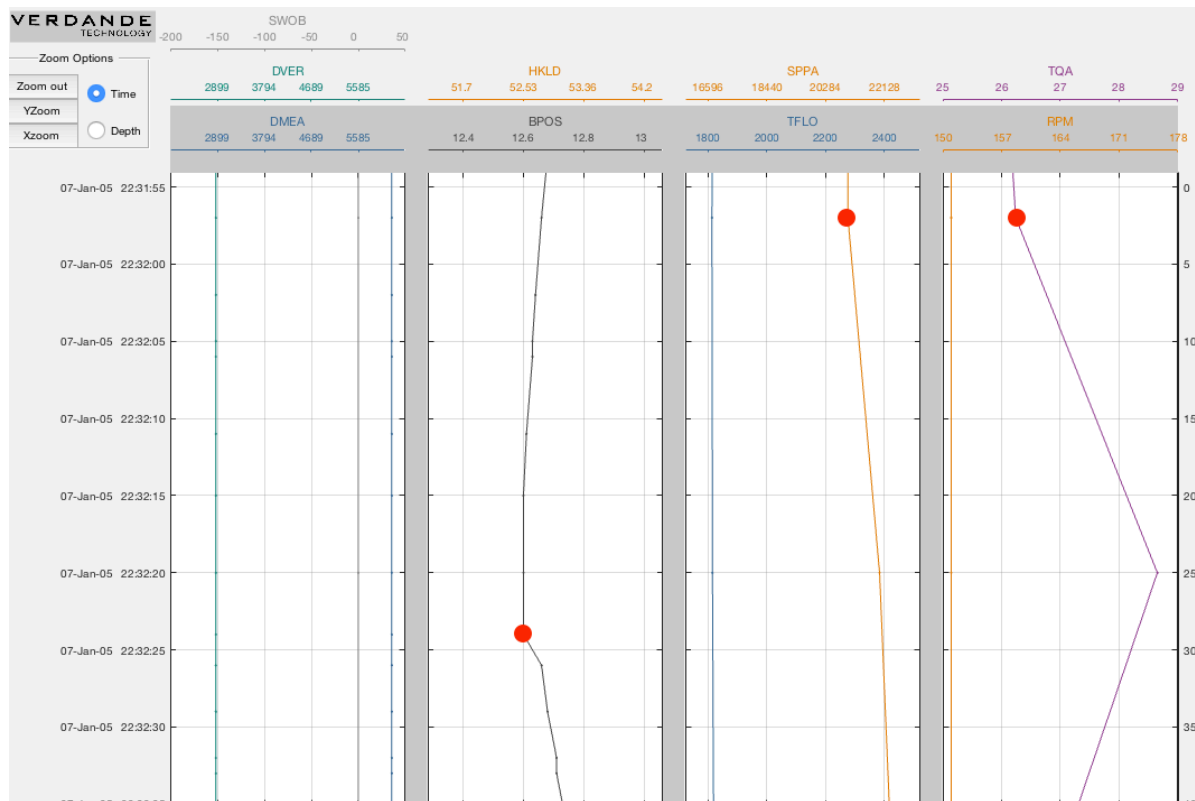


Figure 6.8: Observation of pack-off 07.01.05 at 22:31:57. An increase in TQA is observed at the same time as an increase in SPP. BPOS is a little delayed and is observed after the TQA's peak.

A few cases are found when the alteration in SPP is neither caused by surge, swab or pack-off. An increase or a decrease in WOB and RPM may be the cause of alteration.

Figure 6.9 presents a case where the alteration in SPP is caused by an increase in RPM. An increase or decrease in SPP when there is an increase in RPM is controlled by the annular flow pattern. During the analysis, several incidents of changes in RPM are found.

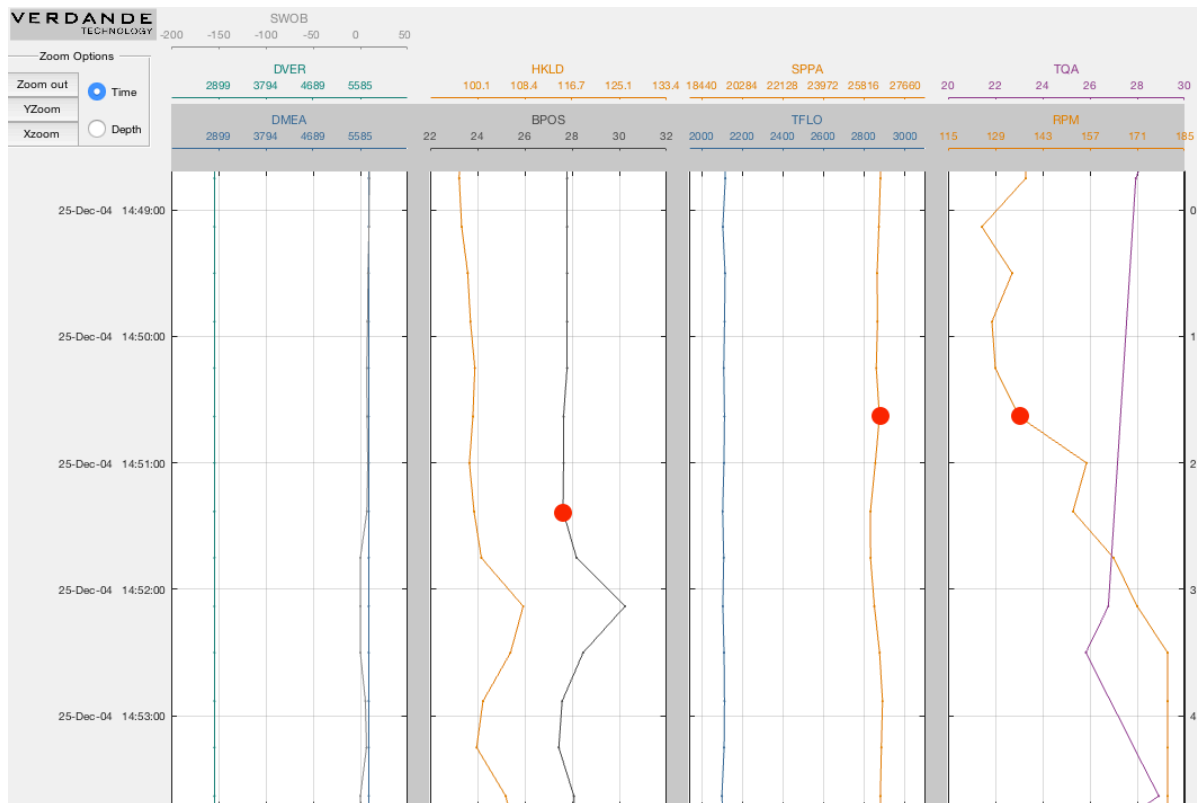


Figure 6.9: Observation of increase in RPM 25.12.04 at 14:15:15. The red circles indicate the beginning of an increase in RPM and a decrease in SPP. The initiation of a BPOS change is also marked on the log.

Figure 6.9 shows field data from the 8 ½" section in well K 480 where RPM is increased. The red circle on the RPM log indicates where RPM starts to increase. The SPP clearly begins to decrease when RPM is increased. Because the block position is increased after the decrease in SPP, surge and swab are not the cause of alteration in SPP.

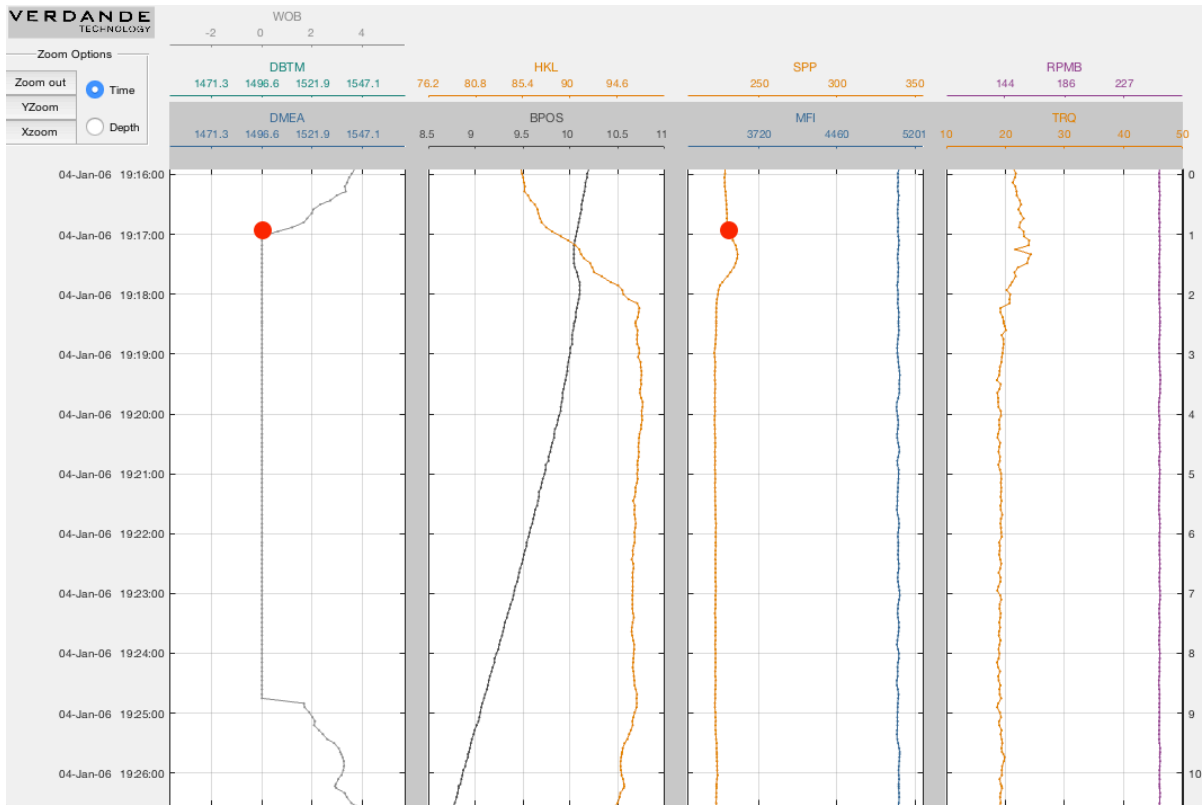


Figure 6.10: Observation of decrease in WOB 04.01.06 at 19:17:00. The reduction in WOB results in an increase in SPP. The other parameters are kept constant at the time WOB is reduced.

A change in WOB can also cause alteration in SPP. Figure 6.10 shows field data from the 17 ½" section in well K 470 where WOB is reduced. The red circles indicate where WOB starts to decrease. There is a correspondingly increase in SPP at the same time as WOB is reduced.

6.2 Field data

In this section, field data is taken from the logs and analyzed. Events of surge and swab are only found in the 8 ½“ section in well K 480. Parameters taken from the field data are used to calculate theoretical surge and swab pressures based on an existing equation. The calculated surge and swab pressure are then compared with the change in SPP from the field data. The results are discussed in the next chapter.

Parameters taken from field data in the logs where events of surge and swab are observed are: time, change in standpipe pressure (Δ SPP), change in block position (Δ BPOS), flow rate (TFLO) and measured depth (DMEA). These parameters are shown in table 6.1 for fourteen cases of surge and swab.

Table 6.1: Field data from analysis of surge and swab in the 8 ½ ” section in well K 480.

Date	Event	Time	Interval	Δ SPP	Δ BPOS	TFLO	DMEA
[dd.mm.yy]		[hh:mm:ss]	[sec]	[bar]	[m]	[l/min]	[m]
26.12.04	Surge	00:11:01	46	238	2.5	1817	5823
26.12.04	Surge	03:22:03	69	266	3.7	2115	5847
26.12.04	Swab	03:23:12	44	689	3.8	2120	5847
26.12.04	Surge	03:23:56	45	698	3.6	2121	5847
26.12.04	Swab	03:24:41	45	461	3.9	2117	5847
02.01.05	Swab	16:37:39	90	575	9.6	1780	6002
03.01.05	Swab	20:45:54	69	728	7.2	1800	6111
03.01.05	Surge	20:47:03	44	762	5.7	1809	6111
03.01.05	Swab	20:47:47	45	889	9.8	1807	6111
03.01.05	Surge	20:48:32	22	651	4.5	1805	6111
04.01.05	Surge	00:28:44	45	397	3.8	2061	6128
04.01.05	Swab	00:29:29	22	387	2.6	2065	6128
04.01.05	Surge	00:29:51	45	595	3.6	2064	6128
04.01.05	Swab	00:30:36	45	688	5	2057	6128

The length of the intervals is in a range of 22-90 seconds, and the corresponding difference in block position varies from 2.5 to 9.8 meters. In the next section equation 6 will be used to calculate surge and swab pressure.

6.3 Theoretical calculations of surge and swab

The existing theory of surge and swab calculations is developed over many years. By looking at articles from different years, the improvement of surge and swab pressure calculations over time can be seen. The yield-power-law model mentioned in this thesis is one of the more recent developments. A lot of simplifying assumptions have been made for this expression, as already mentioned.

Theoretical calculations of the pressure change can be performed by using the surge and swab expression given in equation 6. The field data presented in table 6.1 is used to calculate the parameters shown in table 6.3. Equation 6 depends on the annular fluid velocity. Since surge and swab are observed in the annulus, the hydraulic diameter given in equation 4 is used for more accurate calculations. The annular fluid velocity (v_{ann}) is found from dividing the flow rate by the cross-sectional area of the annulus. Tripping velocity of drillpipe (v_p) can be calculated from change in block position in the given interval over time. The length of the pipe is estimated by subtracting the length of the BHA from the measured depth. The length of the BHA is found from the drilling data and is approximately 122 meter. In order to get a more precise result, the fanning friction factor used in equation 8 has to be calculated for an annulus. The Reynolds' number applied in equation 8 is dependent on both the diameter and the velocity in the annulus. Therefore, the hydraulic diameter is used in the calculations of Reynolds' number and area of annulus. Table 6.2 shows the constant parameters needed for further calculations. The parameters are fluid density, gravity, diameter of the borehole and the outer diameter of the pipe. They are all given in the drilling data.

Table 6.2: Constant input data used in calculations of surge and swab pressure.

Section	ρ [kg/m ³]	g [m/s ²]	d_h [m]	d_p [m]	d_e [m]	ϵ/d_e
K 480 8 1/2"	1570	9.81	0.216	0.127	0.184	0.049

Table 6.3: Calculated parameters for use in calculations of surge and swab pressure.

Date [dd.mm.yy]	Event	Re	f	v_{ann} [m/s]	v_p [m/s]	L_p [m]
26.12.04	Surge	9092	0.0735	1.13	0.0543	5701
26.12.04	Surge	10583	0.0731	1.32	0.0536	5725
26.12.04	Swab	10606	0.0731	1.32	0.0864	5725
26.12.04	Surge	10613	0.0731	1.32	0.0800	5725
26.12.04	Swab	10591	0.0731	1.32	0.0867	5725
02.01.05	Swab	8907	0.0735	1.11	0.1067	5880
03.01.05	Swab	9007	0.0735	1.12	0.1043	5989
03.01.05	Surge	9052	0.0735	1.13	0.1295	5989
03.01.05	Swab	9042	0.0735	1.13	0.2178	5989
03.01.05	Surge	9032	0.0735	1.13	0.2045	5989
04.01.05	Surge	10313	0.0731	1.29	0.0844	6006
04.01.05	Swab	10333	0.0731	1.29	0.1182	6006
04.01.05	Surge	10328	0.0731	1.29	0.0800	6006
04.01.05	Swab	10293	0.0732	1.28	0.1111	6006

The constant and the calculated parameters are then put into equation 6. The resulting calculated surge and swab pressures are shown in table 6.4 together with the difference in SPP found from field data.

Table 6.4: Calculated surge and swab pressures ($\Delta P_{S\&S}$) and standpipe pressure difference (ΔSSP) from field data in the given intervals of surge and swab. The right column shows the difference between the pressures in percentage.

Date [dd.mm.yy]	Event	ΔSSP [bar]	$\Delta P_{S\&S}$ [bar]	$\Delta P_{S\&S}$ of ΔSSP [%]
26.12.04	Surge	238	18.8	7.9
26.12.04	Surge	266	25.7	9.6
26.12.04	Swab	689	28.7	4.2
26.12.04	Surge	698	25.3	3.6
26.12.04	Swab	461	28.6	6.2
02.01.05	Swab	575	21.5	3.7
03.01.05	Swab	728	22.3	3.1
03.01.05	Surge	762	18.3	2.4
03.01.05	Swab	889	24.7	2.8
03.01.05	Surge	651	16.9	2.6
04.01.05	Surge	397	24.9	6.3
04.01.05	Swab	387	29.3	7.6
04.01.05	Surge	595	25.1	4.2
04.01.05	Swab	688	28.9	4.2

The results of calculated surge and swab pressures deviates from the field data. The difference between the pressures are shown in percentage. In the interval where the pressures differ the most, $\Delta P_{S\&S}$ is only 2.4 % of the pressure found in the logs. The best result of comparing the two pressures are 9.6 %. So, the surge and swab pressure calculated by using yield-power-law model is not the same as the standpipe pressure taken from the field data.

7 Discussion

Analysis of field data from logs in four sections from two different wells only gave observations of surge and swab in the 8 ½" section in K480. Fourteen cases of surge and swab are observed in the analyzed sections. There are several reasons why the results from the calculations do not correspond to the field data.

7.1 Analysis of surge and swab

Manually analysis of surge and swab may cause errors. The drilling data shows that hard formations are drilled. The hard formations cause so much problems that a sidetrack has to be drilled. Surge and swab are often observed when problems like this occur. This might be one of the reasons why surge and swab only are observed in well K 480. The drilling data for well K 470 does not show problems like this. In some cases, when the drill bit hits hard formations, the rate of penetration (ROP) and the SPP are reduced. The WOB is increased as more weight is required to maintain ROP. This situation can easily be confused with an event of surge and swab. Analysis of the logs will show an alteration in SPP when the flow rate is kept constant. However, it is necessary to analyze the other parameters in order to not confuse surge and swab with cases of hard formations.

7.2 Parameters taken from the logs

The parameters in the logs are measured at surface. Parameters needed for calculations in equation 6 are estimated based on the parameters measured at surface. These parameters correspond to downhole conditions. Therefore, inaccuracies may be present in the parameters calculated from field data. For example, the calculated tripping speed may diverge from the field data because the bit position is given from the block position at surface. The bit position at a given time may be delayed compared to the block position found in the logs. Measurement errors of the other parameters may also occur. The errors may be caused by delays through the measurement systems.

7.3 Calculation of field data from existing theory

Fourteen intervals of surge and swab are found from the analysis. Calculations of surge and swab pressure from equation 6 do not correspond to the field data. One reason can be that well K 480 and K 470 are drilled in the same oilfield. All of the surge and swab intervals are observed in one well, in the same area. An idea is to analyze other oil fields operated by other companies to get a deeper understanding. Data from other oil fields might show a better coherence between calculated surge and swab pressure and field data. The limited number of intervals reduces the chance of good results.

Many assumptions have been made for the yield-power-law (YPL) model calculations of surge and swab pressure. The YPL model is assumed to be a steady state model that can account for fluid and formation compressibility as well as pipe elasticity (Crespo, 2012). Furthermore, the equation is assumed to apply for turbulent flow as long as the friction factor is calculated as the fanning friction factor. The given assumptions may not be valid for the conditions in the intervals where surge and swab are observed. The well rapport only gives limited information about rheology and geology. Sufficient information will strengthen the quality of the analysis and might give a better result. A better understanding of flow regimes, rheology and hole size in the model could also improve the results. The YPL model assumes a concentric hole, which is often not the case in reality. The eccentricity can lower the calculated surge and swab pressure by 40 %. This will lead to even lower calculated pressures.

7.4 Further work

As mentioned in section 3.4.2, an analytical model has been developed as a lumped element model (Hovda, 2016). The model is considered as a drillstring modelled as a set of n blocks that are connected sequentially by n spring elements. A physical drillstring model is under development to provide the basic understanding needed to simulate and measure the behavior in a drillstring. The expression given in equation 13 for the pressure in the annulus is developed for the analytical model. Equation 14 is motivated from the pressure in the annulus and defines surge and swab pressure. Experimental data is expected to be measured from the physical drillstring. This data will further be used to calculate surge and swab pressure from equation 14. Calculations of surge and swab pressure can then be done for an experiment where the physical drillstring model simulates an event of surge or swab. Hopefully, this will help to give a better understanding of how to prevent surge and swab in a well.

8 Conclusion

Existing theory of surge and swab are compared with field data from four sections in two wells. Surge and swab are only observed in one section. The field data is analyzed through logs, where a rapid alteration in block position at the same time as a change in SPP are an indication of surge and swab. From the analysis the following were concluded:

- Surge and swab events can easily be confused with other events observed in the logs, e.g. hard formation.
- The results calculated with the YPL model did not correspond to the field data. The calculated surge and swab pressures were 9.6 percent of the change in SPP at the best.
- The limited number of intervals reduces the chance of good results. Data from other oil fields might show a better coherence between calculated surge and swab pressure and field data.
- A lot of assumptions are made for the YPL model. The simplifying assumptions, and the possibility of other contributing effects, might explain why the calculated pressures deviate from the field data.
- The need of a physical drillstring model is supported by the inaccurate results obtained from the theoretical equation.

9 Nomenclature and Acronyms

Roman Symbols

A_{ann}	Cross sectional area of annulus
C_1/C_2	Constants
d_e	Hydraulic diameter
d_h	Inner diameter of borehole or casing
d_p	Outer diameter of pipe
f	Fanning friction factor
g	Gravity of Earth
h	Length of segment
L_p	Length of drill pipe
P_{ann}	Wetted perimeter of annulus
P_i	Annular pressure
\dot{q}	Velocity of drillstring
Q	Volumetric flow rate
r	Radius of pipe
R	Radius of borehole
Re	Reynolds' number
u_i	Axial velocity
V	Mud flow
v_{ann}	Average fluid velocity in annulus
v_p	Tripping velocity
z	True vertical depth

Greek Symbols

ΔP	Pressure gradient
ϵ	Absolute roughness of pipe or annulus
$\bar{\epsilon}$	Average absolute roughness of pipe or annulus
ϵ_{oh}	Absolute roughness of borehole
ϵ_p	Absolute roughness of commercial steel in drillpipe
ϵ_{rel}	Relative roughness
μ	General fluid viscosity

ω_d	Damped angular frequency
ρ	General fluid density
ρ_m	Mud density

Acronyms

BHA	Bottom hole assembly
BHP	Bottom hole pressure
BP	Bingham plastic
BPOS	Block position
DDM	Derrick drilling machine
DMEA	Measured depth
MD	Measured depth
PL	Power-law
POOH	Pulling out of hole
ROP	Rate of penetration
RSS	Rotary steerable system
SPP	Standpipe pressure
TFLO	Flow rate
TVD	True vertical depth
TQA	Torque
YPL	Yield-power-law
WOB	Weight on bit

10 References

- CDF Support. (2016, April 08). CDF Support. Retrieved April 08, 2016, from <http://www.cfdsupport.com/OpenFOAM-Training-by-CFD-Support/node263.html>
- Chenevert, M., Bourgoyne Jr., A., Milheim, K., & Young Jr., F. (1986). Applied Drilling Engineering. Society of Petroleum Engineers.
- Cimbala, J., & Cengel, Y. (2014). Fluid Mechanics - Fundamentals and Applications. McGraw Hill.
- Crespo, Freddy; Ahmed, Ramadan; Saasen, Arild; Amani, Mahmood. (2012). Surge-and-Swab Pressure Predictions for Yield-Power-Law Drilling Fluids. SPE Latin American & Caribbean Petroleum Engineering Conference . Lima: SPE.
- Editors of Encyclopædia Britannica. (2016, March 12). Laminar flow. Retrieved March 12, 2016, from Encyclopædia Britannica: <http://global.britannica.com/science/laminar-flow>
- Effendi, S. (2011, June 11). Petroleumsupport. Retrieved April 06, 2016, from <http://petroleumsupport.com/under-balance-drilling-is-a-alternative-for-our-clean-formation/>
- Forutan, M., & Hashemi, A. (2011). The Prediction of Surge and Swab Pressures and Critical Pipe Running Speed While Tripping in a 12 1/4-in hole og Maroun Field in Iran. Petroleum Science and Technology.
- Hovda, S. (2016, May 07). Drill String Models.
- Lake-Bakaar, G., Ahmed, M., Evenson, A., Bonder, A., Faintuch, S., & Sundaram, V. (2015, January 27). Hagen_Poiseuille's law: The link between cirrhosis, liver stiffness, portal hypertension and hepatic decompensation. World Journal of Hepatology .
- Schlumberger. (2016). Schlumberger. Retrieved 05 27, 2016, from Oilfield Glossary: http://www.glossary.oilfield.slb.com/Terms/p/pack_off.aspx
- Serway, R., & Jewett, J. (2009). Physics for Scientists and Engineers.
- Skalle, P., & Mme, U. (2012). Effects of Mud Properties, Hole size, Drill String Tripping Speed and Configurations on Swab and Surge Pressure Magnitude during Drilling Operations. Research India Publications.
- Srivastav, R. (2012, April 16). Surge and Swab Pressures in Horizontal and Inclined Wells. Society of Petroleum Engineers.
- Wold, A., & Kummen, H. (2015). The effect of cuttings on annular pressure loss - An analysis of field data in the North Sea.

Appendix

A Well data

The wells used in this master's thesis are K 470 and K 480 in the North Sea. The data given consist of four sections, three from K 470 and one from K 480. Short summarizing tables of well trajectory, BHA and bit specifications and mud properties are taken from (Wold & Kummen , 2015). Complete information on all the sections is not available. The three sections from well K 470 is 17 ½“, 12 ¼“ and 8 ½“, and from well K 480 , the 8 ½ “ is the only section. Drilling data is available for all sections. Well trajectories for both wells are plotted in figure D.1 and D.2.

A.1 Well K 470

17 ½“ section

Section geometry	
TVD interval	1316-1709 mTVD
MD interval	1508-2379 mMD
Interval length	871 m
Inclination start	60.8
Inclination end	60.4
Azimuth start	134.7
Azimuth end	99.1

BHA and bit	
Drillpipe	6 5/8”
Length of BHA	107 m
Steering	Power Drive
Bit	17 ½ ” milled tooth

Mud	water based
------------	-------------

Mud weight	1300 kg/m ³
Average plastic viscosity	- mPas
Average yield point	- Pa
Average Power law exponent	- [-]
Average consistency index	- lbf s ⁿ /100ft ²

12 ¼“

Section geometry

TVD interval	2821-2895 mTVD
MD interval	2879-2787 mMD
Interval length	408 m
Inclination start	70.4
Inclination end	81.9
Azimuth start	81.5
Azimuth end	351.5

BHA and bit

Drillpipe	5”
Length of BHA	64 m
RSS	Motor and SRWD
Bit	8 ½“ PDC with 10 5/8” X 12 ¼” reamer wing

Mud

Mud weight	1300 kg/m ³
Average plastic viscosity	- mPas
Average yield point	- Pa
Average Power law exponent	- [-]
Average consistency index	- lbf s ⁿ /100ft ²

8 ½“ section

Section geometry

TVD interval	1911-2072 mTVD
MD interval	2787-4399 mMD
Interval length	1512 m
Inclination start	63
Inclination end	94
Azimuth start	105
Azimuth end	180

BHA and bit

Drillpipe	5”
Length of BHA	39 m
RSS	PowerDrive Xceed
Bit	8½” PDC

Mud

Mud weight	1700 kg/m ³
Average plastic viscosity	- mPas
Average yield point	- Pa
Average Power law exponent	- [-]
Average consistency index	- lbf s ⁿ /100ft ²

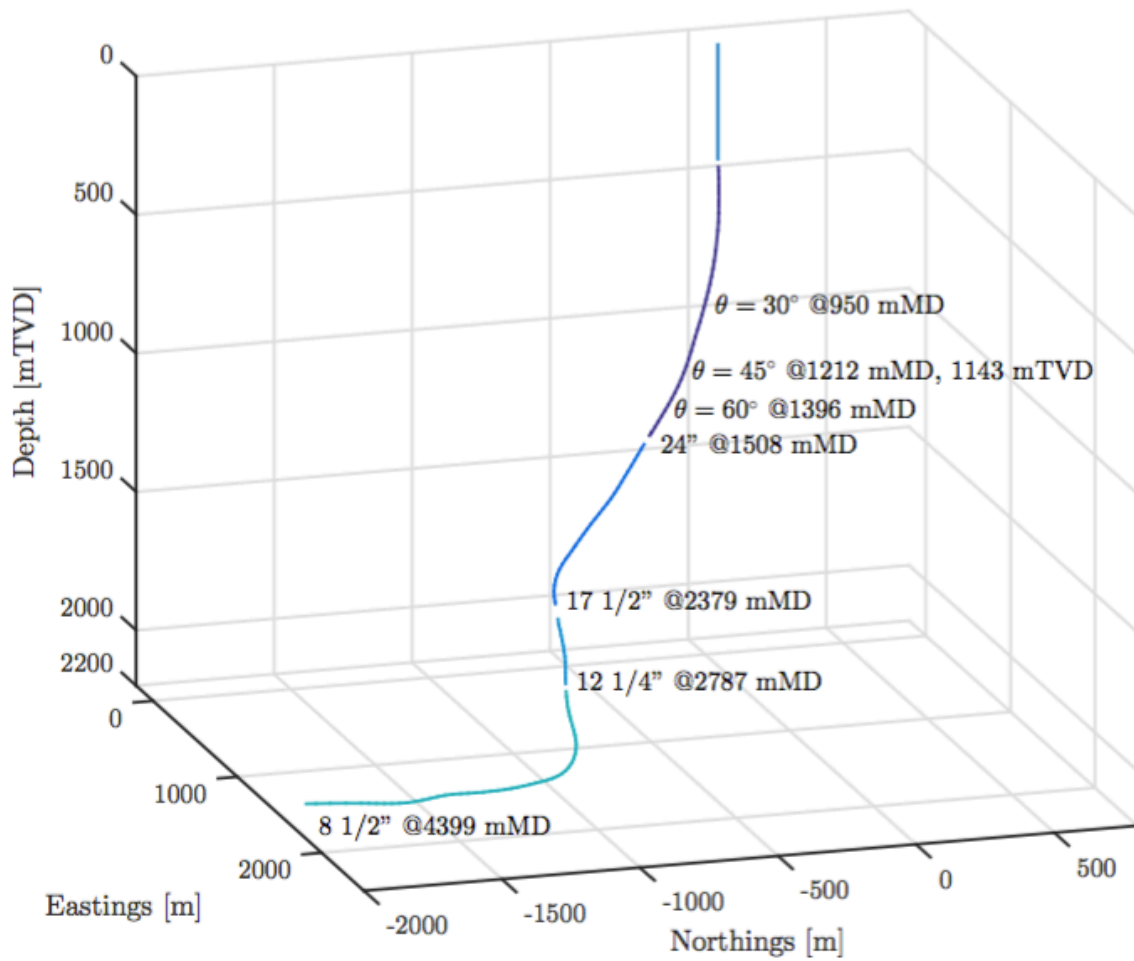


Figure A-1: Survey of well K 470 (Wold & Kummen , 2015).

A.2 Well K 480

8 ½“

Section geometry

TVD interval	2821-2895 mTVD
MD interval	5091-6221 mMD
Interval length	1130 m
Inclination start	70.4
Inclination end	81.9
Azimuth start	81.5
Azimuth end	351.5

BHA and bit

Drillpipe	5"
Length of BHA	122 m
RSS	PowerDrive Xceed
Bit	8½" PDC

Mud

Mud weight	1570 kg/m ³
Average plastic viscosity	36.1 mPas
Average yield point	12.4 Pa
Average Power law exponent	0.68 [-]
Average consistency index	4.85 lbf s ⁿ /100ft ²

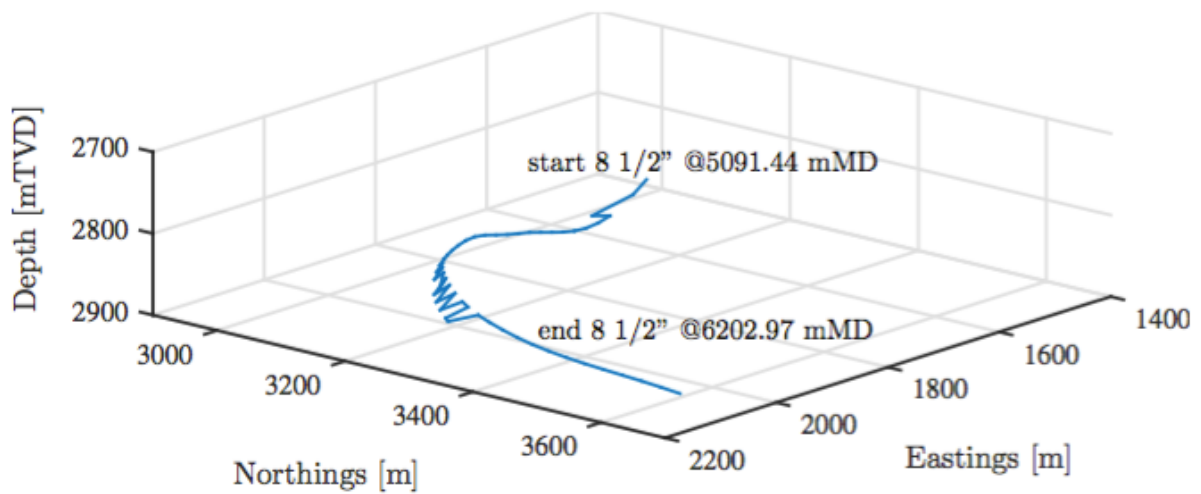


Figure A - 2: Survey of well K 470 (Wold & Kummen , 2015).

B Logs used for analysis

Overview of the logs used in the analysis of surge and swab.

B.1 Well K 470

17 ½" section

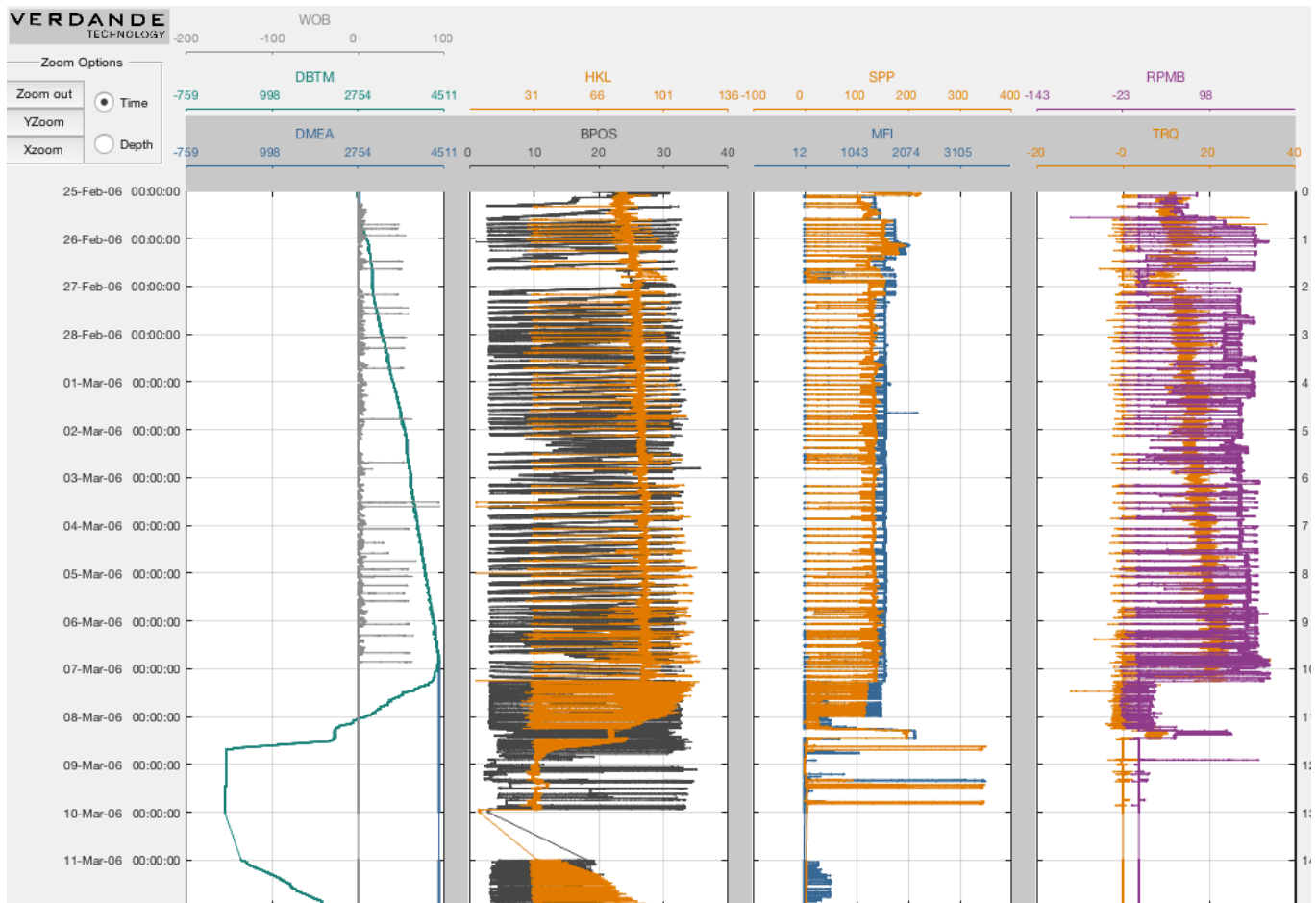


Figure B-1: Overview of the log used for analysing 17 ½" section in well K 470

12 ¼" section

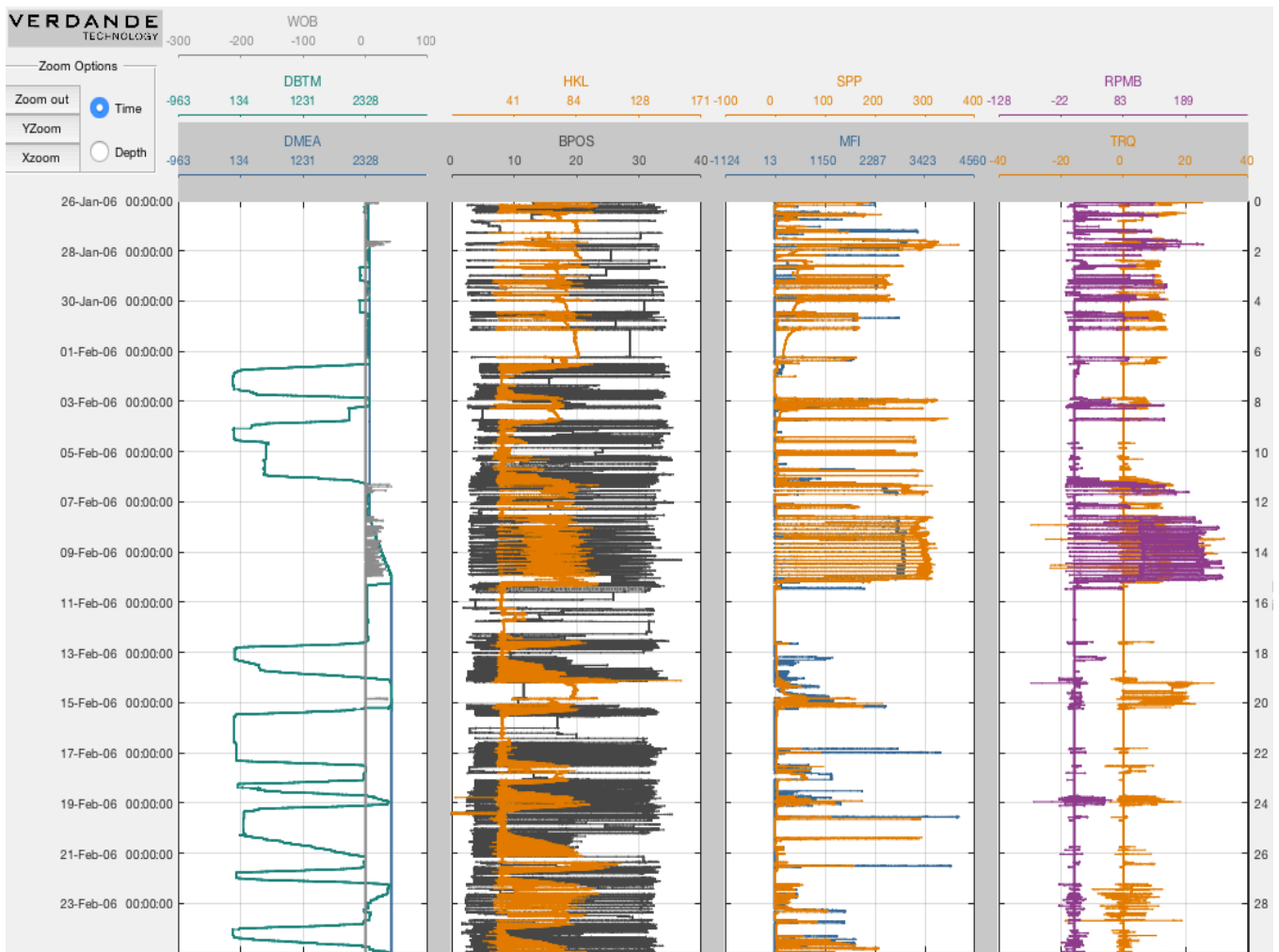


Figure B-2: Overview of the log used for analysing 12 ¼" section in well K 470

8 1/2" section

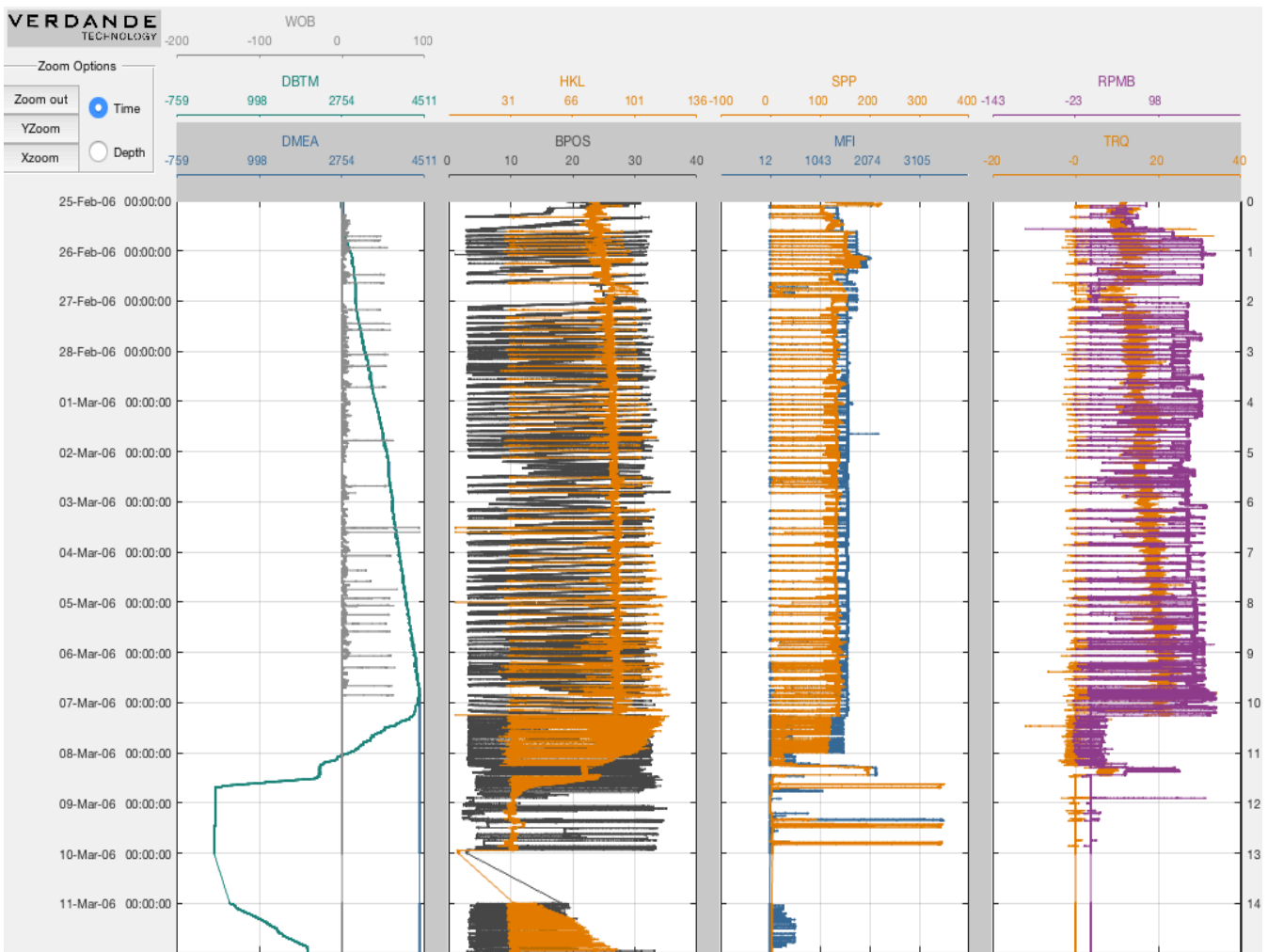


Figure B-3: Overview of the log used for analysing 8 1/2" section in well K 470

B.2 Well K 480

8 ½" section

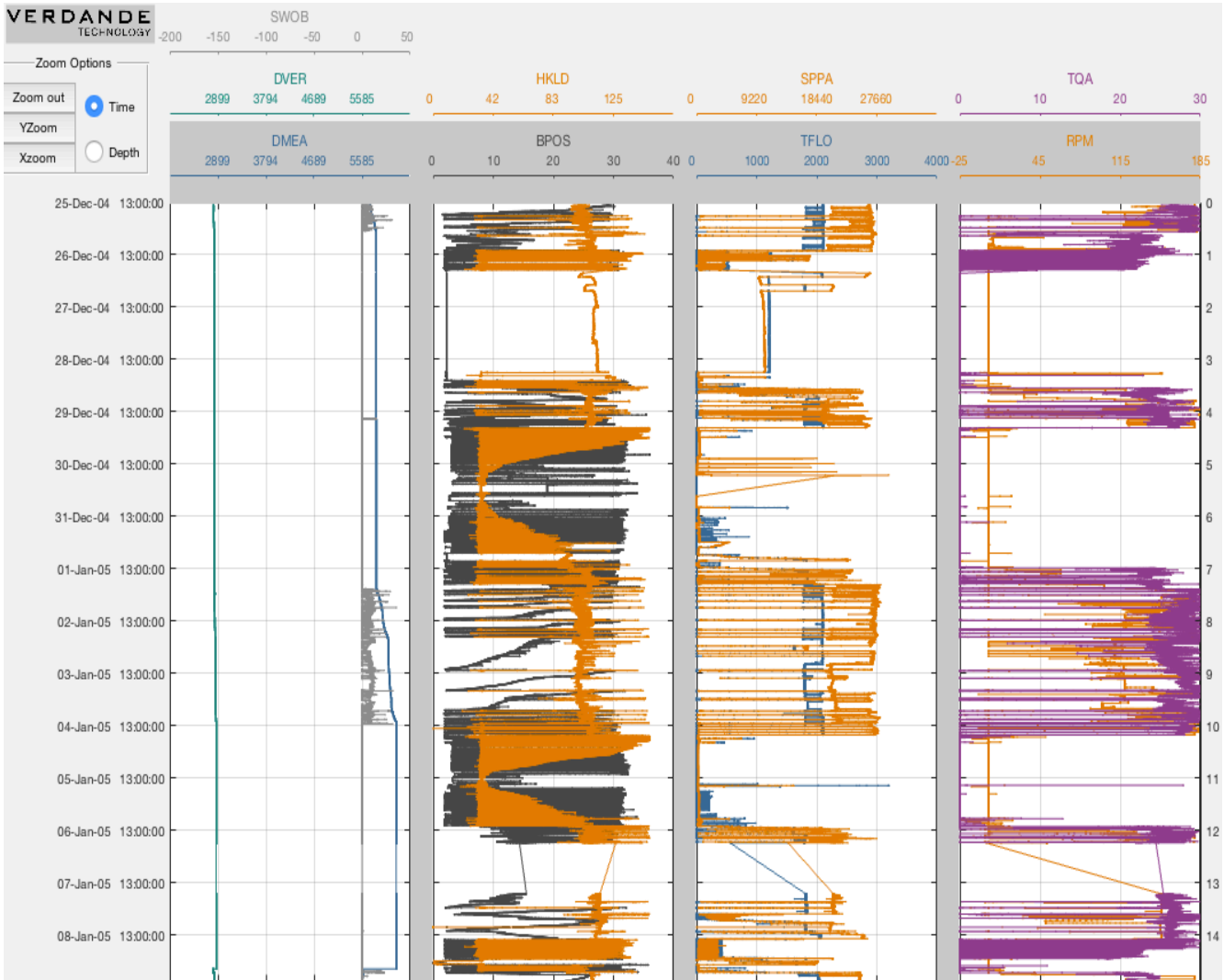


Figure B-4: Overview of the log used for analysing 8 ½" section in well K 480